ac and dc conductivity, magnetoresistance, and scaling in cellular percolation systems

C. Chiteme and D. S. McLachlan
School of Physics and Materials Physics Institute, University of the Witwatersrand, Johannesburg 2050, South Africa
(Received 8 May 2002; published 29 January 2003)

Percolation phenomena, which include the ac and dc conductivity, dielectric constant, and magnetoresistance, are studied in a series of seven cellular composites, consisting of small conductor particles embedded on the surface of larger insulator particles. Carbon black (ground and unground), graphite, graphite–boron-nitride, niobium carbide, nickel, and magnetite (Fe_3O_4) powders were the conducting components with talc-wax powder as the common insulating component. The dc conductivity results were fitted to the standard percolation equations and to a two-exponent phenomenological equation, which yields the percolation parameters σ_i, σ_c, s, t, and ϕ_c in the ideal limits. Both universal and nonuniversal values of s and t are measured in the systems. Close to the percolation threshold (ϕ_c), the ac conductivity (σ_{mr}) and the dielectric constant (ε_{mr}) are found to scale as $\sigma_{mr} \propto \omega^u$ and $\varepsilon_{mr} \propto \omega^{-v}$. All these exponents are examined using the most recent theories and compared with previous studies. The dielectric constant exponent (s'), from $\epsilon_{mr} \propto (\phi_c - \phi)^{-s'}$, is shown to be frequency dependent. The exponents g_c (magnetoresistance) and t_m (from magnetoconductivity) in composites are not yet clearly understood but these and previous results show that $t_m > t$. dc scaling is shown in a real composite comprising Fe_3O_4 and talc wax.

DOI: 10.1103/PhysRevB.67.024206 PACS number(s): 72.60.+g, 72.20.My, 71.30.+h, 72.80.Tm

I. INTRODUCTION

The properties of conductor-insulator (or metal-insulator) composites have been extensively studied by both experimental and theoretical physicists for many years. At first mixture rules and later effective media theories[1,2] were used to analyze the data, but since the 1970s, one of the main theoretical models has involved percolation theory and the concept of scaling. This was due to the realization that the percolation threshold in metal-insulator systems (lattice models, model systems, and continuum composites) is a critical point, analogous to the critical points of second-order phase transitions in thermodynamic systems. Major review articles covering ''standard'' percolation theory, scaling, and some experimental results are given in Refs. 3–5. Most of the experimental work has been focused on the simple dc resistivity properties, less on the ac dielectric or conductivity properties, the Hall effect, and flicker noise, and very little on the magnetoresistivity and thermopower. In most experimental papers only one or two of these properties was measured on the same system, which makes it difficult to compare and correlate the different exponents that appear in the various scaling laws, which often have the form $Q \propto (\phi - \phi_c)^x$, while the real conductivity $[\sigma_{mr}(\omega)]$ and dielectric constant $[\varepsilon_{mr}(\omega)]$ are found to scale as $\sigma_{mr} \propto \omega^u$ and $\varepsilon_{mr} \propto \omega^{-v}$. Here Q is the physical (electrical) property measured, x, u, and v the (in some cases universal) exponents, ϕ the volume fraction of the conducting component, and ϕ_c the critical volume fraction, where the conducting component first forms an infinite or spanning cluster in the sample or a continuous dc conduction path across an infinite (in practice very large) sample. This paper reports on measurements of the dc conductivity exponents s and t and the ac exponents u and v, together with the ϕ_c value, in seven percolation systems and then tries to relate them to the theoretically predicted values and those measured in other percolation systems. Studies of the power-law dependence of the dielectric constant below ϕ_c are made, and the exponent s' from $\epsilon_{mr} \propto (\phi_c - \phi)^{-s'}$ is found to be frequency dependent. The ac conductivity results are scaled and analyzed in a way similar to those reported in Ref. 6 using, where possible, the exponents obtained from the dc results.

Up until nearly ten years ago it was widely believed that all exponents, whether measured in a lattice model (computer simulation), a model system, or a continuum composite, were universal, in that they depended on the geometrical dimension only–three dimensions (3D) in these experiments. Since then, it has been realized that there are a number of continuum systems in which unequivocal nonuniversal exponents have been observed or predicted (Refs. 6 and 7 and references therein). Many of the exponents presented in this paper are nonuniversal and will be discussed using the currently accepted models for nonuniversal exponents (see theory section).

II. THEORY

In analyzing the data the equation used is[6–10]

$$(1-\phi)(\sigma_i^{1/s} - \sigma_m^{1/s})/(\sigma_i^{1/s} + A\sigma_m^{1/s}) + \phi(\sigma_c^{1/t} - \sigma_m^{1/t})/(\sigma_c^{1/t} + A\sigma_m^{1/t}) = 0. \quad (1)$$

This gives a phenomenological relationship between σ_c, σ_i, and σ_m, which are the conductivities of conducting and insulating component and the mixture of the two components, respectively. Note that all three quantities σ_c, σ_i, and σ_m can be real or complex numbers in Eq. (1). The conducting volume fraction ϕ ranges between 0 and 1 with $\phi = 0$ characterizing the pure insulator substance ($\sigma_m \equiv \sigma_i$) and $\phi = 1$ the pure conductor substance ($\sigma_m \equiv \sigma_c$). The critical volume fraction or percolation threshold is denoted by ϕ_c, where a transition from an essentially insulating to an essen-

tially conducting medium takes place, and $A=(1-\phi_c)/\phi_c$. Equation (1) yields two limits

$$|\sigma_c|\to\infty: \quad \sigma_m=\sigma_i[\phi_c^s/(\phi_c-\phi)^s], \quad \Phi<\phi_c, \tag{2}$$

$$|\sigma_i|\to 0: \quad \sigma_m=\sigma_c[(\phi-\phi_c)^t/(1-\phi_c)^t], \quad \phi>\phi_c, \tag{3}$$

which chararcterize the exponents *s* and *t*. Note that Eqs. (2) and (3) are the normalized percolation equations. In the crossover region, where ϕ lies between $\phi_c-(\sigma_i/\sigma_c)^{1/(s+t)}$ and $\phi_c+(\sigma_i/\sigma_c)^{1/(s+t)}$,[3–5] Eq. (1) gives

$$\sigma_m\approx\sigma_i^{s/(s+t)}\sigma_c^{t/(s+t)}, \tag{4}$$

in agreement with the theory given in Refs. 3–5.

The scaling functions used in this paper, based on those given in Refs. 3–5, are

$$\sigma_m=\sigma_c[(\phi_c-\phi)^t/\phi_c^t]F_-(x_-), \quad \phi<\phi_c, \tag{5}$$

$$\sigma_m=\sigma_c[(\phi-\phi_c)^t/(1-\phi_c)^t]F_+(x_+), \quad \phi>\phi_c, \tag{6}$$

where σ_m can be the theoretical result from Eq. (1) or the experimental results. The scaling functions $F_\pm(x_\pm)$ depend on the scaling parameters[6]

$$x_-=(\sigma_i/\sigma_c)[(\phi_c^{s+t}/(\phi_c-\phi)^{s+t}]=-i\omega/\omega_{c-}, \quad \phi<\phi_c, \tag{7}$$

with

$$\omega_{c-}=(\sigma_c/\varepsilon_0\varepsilon_i)[(\phi_c-\phi)^{s+t}/\phi_c^{s+t}]$$

and

$$x_+=(\sigma_i/\sigma_c)[(1-\phi_c)^{s+t}/(\phi-\phi_c)^{s+t}]=-i\omega/\omega_{c+}, \quad \phi>\phi_c, \tag{8}$$

with

$$\omega_{c+}=(\sigma_c/\varepsilon_0\varepsilon_i)[(\phi-\phi_c)^{s+t}/(1-\phi_c)^{s+t}] \quad [\propto\sigma_m(\phi,0)^{(s+t)/t}].$$

The above expressions for $\omega_{c_\pm}$ assume a purely real $\sigma_c(\sigma_{ci}=0)$ and imaginary $\sigma_i(\sigma_{ii}=-\omega\varepsilon_0\varepsilon_i, \sigma_{ir}=0)$, as was done in Refs. 3–6. To ensure that curves drawn for $F_\pm$ fall on top of each other for different ϕ_c values, the normalization employed in this paper differs slightly from the one used in Refs. 3–5.

The results for the slopes of the scaling functions $\mathrm{Re}\,F_-$, $\mathrm{Im}\,F_-$ and $\mathrm{Re}\,F_+$, $\mathrm{Im}\,F_+$ and conductivity power laws (exponents) from standard percolation theory, as given in Refs. 3–5, and those from Eqs. (1), (5), and (6) (Refs. 6, 8, and 10) are all the same when x_- and $x_+>1$ and so too are the slopes of the first-order terms $\mathrm{Im}\,F_-(x_-<1)$ and $\mathrm{Re}\,F_+(x_+<1)$. However, the second-order terms of the complex functions F_+ (i.e., $\mathrm{Im}\,F_+$) and F_- (i.e., $\mathrm{Re}\,F_-$) [or $\sigma_{mi}(\phi>\phi_c)$ and $\sigma_{mr}(\phi<\phi_c)$] differ from those given in Refs. 3–5 when $x_+(\omega/\omega_{c+})<1$ and $x_-(\omega/\omega_{c-})<1$. This has been shown analytically in Ref. 8, where experimental measurements of $\sigma_{mi}(\phi>\phi_c)$ and $\sigma_{mr}(\phi<\phi_c)$, which help to resolve this dilemma, have also been reported. The previously defined crossover region now corresponds to x_+ and $x_->1$.

At first it was believed that simulations, based on resistance networks, and real continuum media both belonged to the same universal class and that *s* and *t* depended on the dimension of the system only. The most widely accepted universal dc exponents, in three dimensions, are $s_{un}\approx 0.87$ and $t_{un}\approx 2.0$, but values of *t* down to 1.7 are often taken to be acceptable. All computer simulations and many continuum systems supported this belief, but it was also found, in a number of continuum systems, that *t* was 3 or even larger.

Kogut and Straley[11] were the first to show that if the low-conductance (*g*) bonds in a percolating resistor network had a distribution $h(g)$, characterized by $h(g)\approx g^{-\alpha}$ with $0<\alpha<1$, then the conductivity exponent *t* would be given by

$$t=t_{un}+\alpha/(1-\alpha), \quad 0<\alpha<1, \tag{9}$$

while for $\alpha<0$, $t=t_{un}$ where t_{un} is the accepted universal value. For a superconductor-normal resistor network ($\sigma_c\to\infty$ and σ_i finite), with the distribution of normal conductances (now in the σ_i component) being characterized by $j(g)\approx g^{-\beta}$, the exponent *s* would be given by[11]

$$s=s_{un}+(2-\beta)/(\beta-1), \quad 1<\beta<2, \tag{10}$$

while for $\beta>2$, $s=s_{un}$. Note that this model does not allow either *s* or *t* to be lower than the accepted universal values of s_{un} and t_{un}. While values of $t<t_{un}$ are uncommon, values of $s<s_{un}$ are often observed, especially in ac dielectric experiments.

The first model to propose a distribution of the $g^{-\alpha}$ class, leading to a nonuniversal *t* in a continuum system, was the "Swiss-cheese" or random void (RV) model[3,4,12,13] where the narrow conducting necks, joining the larger regions of the conducting material, dominate the resistive behavior. This class of system was realized by Lee *et al.*[14] in a system of glass spheres randomly distributed in indium and gave $t=3.1$. However, the inverse random void model or inverted "Swiss-cheese" system, where lumps of the conducting phase are separated by noncontinuous thin sheets of insulator, gave a universal exponent.[14] The upper and lower limits of *t* for the RV (Swiss-cheese) model are 2.5 and 2.00, respectively.

Balberg[15,16] proposed a model which accounts for values of *t* higher than those allowed by the RV and the inverse random void (IRV) model.[12,13] In this model Balberg assumes that the resistance distribution function $h(\varepsilon)$, where ε is the proximity parameter, has the form $\varepsilon^{-\omega'}$ as $\varepsilon\to 0$ (where $-\infty<\omega'<1$) and does not tend towards a constant as in the original RV and IRV models.[12,13] Using the approach of Refs. 12 and 13 and keeping the underlying nodes, links, and blobs model,[17,18] Balberg derived an expression for a nonuniversal *t*:

$$t=t_{un}+(u+\omega'-1)/(1-\omega'). \tag{11}$$

For $\omega'=0$, the expression gives the original Halperin-Feng-Sen and Tremblay-Feng-Breton models[12–14] with 2.5 as an

upper limit for t. The parameter u is related to the dimensionality d of the system and is such that $u=d-3/2$ for the RV (Swiss-cheese) model and $u=d/2-1$ for the IRV (inverse-Swiss-cheese) model. Different combinations of ω' and u will give various values of the exponent t in the Balberg model. There appears to be no upper limit to t in this model.

Another model that may allow t values of somewhat greater than 2 is the Links-Nodes-Blobs (LNB) model of Stanley[19] and Coniglio,[20] which supercedes the oversimplied links-nodes model of de Gennes[17] and Skal and Shklovskii,[18] and provides a realistic picture of the backbone on a lattice and enables the critical exponents to be calculated or estimated. In this picture, a node is any site on the backbone that is connected to the boundaries by at least three independent paths and the internode spacing, above ϕ_c, is the correlation length $\xi \approx (p-p_c)^{-\nu}$ [$\equiv(\phi-\phi_c)^{-\nu}$ in a continuum]. A link consists of lengths of single or cutting bonds (i.e., those which, if cut, will interrupt the current flow) and blobs (which are multiply connected paths on the backbone, where each path carries a fraction of the backbone current). The average resistance between two sites, separated by the percolation correlation length ξ, is $\propto(p-p_c)^{-\delta}$, which leads to the expression $t=\delta+(d-2)\nu$.[19,20] According to Refs. 20 and 21, the random resistor model gives $\delta=1.12$ in 3D, which leads to $t=1.95$ [with $\delta=1.12$ and $\nu=0.83$ (Ref. 21)]. To account for the larger t, which is found in some continuum systems, δ would have to be larger than 1.12 (which implies a large fraction of blobs on the backbone). Fisch and Harris[21] gave the limit $\nu<\delta<\nu/\nu_s$, where ν_s is the correlation length exponent for self-avoiding walks. Using their values of $\nu=0.83$ and $\nu_s=0.588$, this gives δ an upper limit of 1.49. Note that ν values of 0.83–0.89 have been put forward. Therefore, in its current form, the LNB model is unable to account for t values higher than about 2.35 unless the complexities of the links, nodes, and blobs in a system of real grains (with the possibility of an anisotropic or shape dependent conductivity and a range of intergrain conductances) allow δ to be higher than 1.49.

Balberg[15,16] also proposed a model similar to the Swiss-cheese model, but where the interparticle conduction method is tunneling. This leads to a large range of interparticle resistances and nonuniveral t values. A large range of interparticle contact resistances could also arise from angular conducting powders, where pointed corners make contact with more planar surfaces. In such systems a wide range of the areas of and pressures on the point contacts would lead to a wide range of resistances and nonuniversal t values. There is, in principle, no upper limit to the t exponent which depends only on the distances between the grains.

Note that the models discussed in Eqs. (9)–(11) and the LNB model are for a homogeneous (nongranular) conducting component, while the tunneling model obviously deals with a granular conducting component. As the ''macroscopic'' geometry of the cellular systems discussed in this paper is similar to that of the RV model, the conducting powders on the insulating grains have an LNB structure and there is tunneling and high-resistance-pressure contacts between the grains; all these existing models have to be considered. Unfortunately the RV and LNB models have not been extended to media with a granular conducting component.

The phenomenon of magnetoresistance or magnetoconductivity has not been extensively studied in percolation systems. To the authors' best knowledge, there has been essentially two theoretical papers[22,23] and three experimental studies.[7,24,25] Bergman[22] used a scaling approach to develop expressions for the low-field Hall effect and magnetoresistance. In systems where $\sigma_c \gg \sigma_i$, it is predicted that the change in conductivity $\Delta\sigma$ $[=\sigma(0)-\sigma(H)] \propto H^2$ and

$$\Delta\sigma \propto (\phi-\phi_c)^{t_m}. \tag{12}$$

In addition, the relative magnetoresistance $[(R(H)-R(0)]/R(0) \propto H^2$ and

$$[R(H)-R(0)]/R(0) \propto (\phi-\phi_c)^{g_c}, \tag{13}$$

where t_m and g_c are critical exponents, H is the magnetic field, and R is the sample resistance.[22]

III. EXPERIMENTAL PROCEDURE

Several conducting powders [graphite (G: Lonza, KS75), carbon black (CB: Raven 430 ultra powder, Columbian Chemicals Co.), niobium carbide (NbC: 51101, 99+%, Johnson Matthey, GMBH Alfa products, $\sim$1–3 μm), magnetite (Fe_3O_4: 97%-325 mesh, Johnson Matthey GmBH Alfa), and nickel, (NI: CERAC, 99.9% pure, $\sim$5 μm average)] were each mixed with spherical talc-wax powder (with an average diameter of 300 μm), coated with 4% wax by volume, which was used as the common insulating component. Note that the particle sizes quoted above for the conducting powders are those specified by the manufacturers. The conductor particles were deliberately chosen to be much smaller than the talc-wax particles so that the conductor particles formed the surfaces of ''bubbles,'' surrounding the insulator particles (voids)—i.e., a three-dimensional ''cellular'' structure. As a result, the conductor particles had the same macroscopic distribution in all systems. The powders were mixed in a way that ensured even distribution of the conductor particles on the surface of the insulator. The graphite–boron-nitride–talc-wax system is a three-component system in which the talc wax is always coated by a mixture of graphite and boron nitride powders, whose combined volume fraction is fixed at $\phi_{GBN}=0.15$ and the graphite content was varied between 0.00 and 0.15. Note that the graphite and boron nitride powders used in the present study are the same as those used in Refs. 6 and 7.

The powders (with the exception of the talc wax, nickel, niobium carbide, and the ''unground'' or ''raw'' carbon black) were initially ground in a planetary mill (in an agate crucible with agate balls) down to a mean size between 9 and 35 μm, before being examined using a JSM 840 scanning electron microscope. Images were obtained at various magnifications in order to estimate the size and shape of the particles. The principle use of the electron microscopy results was not to size, but to observe the particle shapes, as the latter play a role in the determination of the percolation threshold. A Malvern size analyzer was used to measure the

particle size distribution of the powders. The Malvern instrument uses a light-scattering method to measure the various powder particle size, using the light from a helium-neon laser ($\lambda \sim 0.63\ \mu$m). The instrument has two ways of describing the particle size: the mean diameter (D_m) and the sauter diameter (D_s). The sauter diameter is obtained by considering the surface area covered by the particle, while the mean diameter is calculated from the equivalent spherical volume of the particle. These parameters are given and discussed in the next section.

Samples were prepared by first mixing the preweighed conducting and insulating powders by hand. A planetary mill, without the grinding balls, was used to further mix the soft conducting powders (carbon black, graphite, and graphite–boron-nitride powders) for 20 min. The harder and/or heavier powders (niobium carbide, nickel, and Fe_3O_4) were mixed by putting the hand-mixed powders in a bottle (with rods running parallel to its axis) which in turn was put in a slowly rotating drum in which the mixture was tumbled for 20 min. About 4 g of each mixture were gently poured into a die and compressed into a pellet of 26 mm diameter and about 3 mm thickness, at a pressure of 380 MPa, for 1.5 h. This caused the coated talc-wax particles to have a flattened sphere shape, with a height typically half the diameter. The porosity was determined from the measured apparent density, obtained from the actual mass and volume of the pellets, and the calculated fully compacted density. This, together with the conductor volume fraction, was used to determine the volume fraction (ϕ) of the conducting component in each sample, the porosity being added to the insulator fraction ($1-\phi$). Near the percolation threshold, the conductor fraction was varied in 0.2% increments so as to resolve the details of the divergence of the properties under study near ϕ_c. Resistance measurements were done in both a 2 and a pseudo-4-probe configuration, using the two copper wire spirals embedded in each of the silver paint ''capacitor'' plates on the flat surfaces of the disks. Later, for the high-frequency measurements, disks were drilled out with a diameter of 10 mm and polished to a thickness of about 1.5 mm for insertion in the sample holder of the high-frequency impedance analyzer.

Two-terminal conductivity measurements for samples with resistances between 10^5 and $10^{13}\ \Omega$ were made at room temperature (22°C) using a Keithley 617 electrometer in the V/I mode, which had been calibrated using standard resistors. All measurements were done with the sample placed in a shielded Faraday box to reduce external noise. Samples on the conducting side (10^{-3}–$10^5\ \Omega$) were measured using a LR400 self-balancing four-terminal bridge, which was precalibrated using standard resistors in the appropriate ranges. The measured dc resistances were divided by the appropriate geometric factors to obtain the respective dc conductivities, which were then plotted as logarithmic conductivity versus the conducting powder volume fraction (ϕ). The results were fitted to both the combined percolation equations and Eq. (1) to obtain s, t, σ_c, σ_i, and ϕ_c. The uncertainty in these parameters were given by the statistics report of the Micromath Scientist fitting package. The first measurements of the dc resistance were made within 24 h of making the sample. No significant change in the resistance was observed after this, but to be absolutely sure all reported results are from measurements taken at least 2 months after the first measurements as was done in Ref. 7. The samples were kept in dessicators, filled with silica gel, to guard against contamination by moisture, which would have resulted from prolonged exposure to the atmosphere and all measurements were done on relatively dry days.

Magnetoresistance measurements were made on the 10-mm-diam samples (which had been drilled out of the 26-mm-diam samples and polished to about 1.5 mm thickness) on five of the systems [RCB, GCB, GG, GBN, and NI (see caption to Table I for the full names)]. All measurements were done at room temperature using a LR400 self-balancing bridge for measuring the resistance at each field setting. A Hewlett-Packard 6438B supplied current to a Newport electromagnet whose field could be adjusted from 300 to 15 000 G, as measured using a LakeShore 450 gaussmeter. All samples used in the measurements were in the conducting region ($\phi > \phi_c$).

Low-frequency ac measurements were done using a Novocontrol Dielectric Spectrometer, in combination with a Solartron SI1260 Impedance Analyzer. The Novocontrol Dielectric Spectrometer, which is an instrument especially designed for ac conductivity measurements and works from the subhertz to megahertz range, is capable of measuring far smaller loss components in the dielectric or insulating phase (equivalent to $10^{14}\ \Omega$ at 10^{-2} Hz and $10^8\ \Omega$ at 100 kHz in parallel with an ideal capacitor) and has a better resolution of the loss or phase angle (a maximum of $\tan\delta$ of $>10^3$ and a minimum of 10^{-3}) than the instruments used in Ref. 6 or any previous measurements of a similar nature. The capacitor areas were chosen so that the capacitance and resistance of the sample were, where possible, well within the measurement limitations (capacitance, resistance, and $\tan\delta$) of the dielectric spectrometer.

The high-frequency measurements (from 1 MHz to 1.8 GHz) were done on a Novocontrol BDS 6000 impedance analyzer, which consisted of a HP 4291A rf impedance analyzer, a Novocontrol sample holder, and a Novocontrol WINDETA Software package. After carrying out the calibration procedure, the samples were inserted between the plates in the sample holder, which placed them at the termination of a coaxial line. The experiments were carried out under the control of the WINDETA package and the results could be plotted out and stored as the real and imaginary conductivity, impedance, or dielectric constant or $\tan\delta$ as a function of frequency.

The results from the two spectrometers overlapped in the range 1–10 MHz. As the results in this region seldom coincided perfectly, the results from the high-frequency spectrometer were scaled to coincide with those of the low-frequency spectrometer in this range.

IV. RESULTS AND DISCUSSION

The results obtained from the measurements and the discussion of the parameters obtained from the analysis of these results are presented in the following order: (a) The dc con-

TABLE I. Percolation parameters from the cellular systems. The abbreviations used represent GCB, ground carbon black; GG, ground graphite; Fe_3O_4, Magnetite; NI, nickel; RCB, raw carbon black, GBN, graphite/boron nitride; NbC, niobium carbide. The numbers in brackets represent the corresponding statistical errors except in the σ_{cf} and σ_{cb} rows where they denote corresponding powers of 10. Note also that due to space constraints, the last significant figure has been omitted in the ϕ_{ce} values for the GCB and RCB systems, which are 0.0122 ± 0.0007 and 0.0131 ± 0.0006, respectively.

	GCB	RCB	GG	GBN	Fe_3O_4	NbC	NI
ϕ_{cs}	0.032(0.001)	0.045(0.001)	0.09(0.01)	0.034(0.001)	0.030(0.001)	0.06(0.01)	0.07(0.01)
ϕ_{cm}	0.020(0.005)	0.028(0.005)	0.08(0.01)	0.025(0.001)	0.025(0.001)	0.009(0.001)	0.040(0.001)
ϕ_{ce}	0.012(0.001)	0.013(0.001)	0.035(0.002)	0.033(0.001)	0.025(0.003)	0.065(0.003)	0.025(0.005)
t	2.06(0.10)	2.26(0.11)	1.93(0.06)	2.51(0.12)	4.12(0.23)	5.25(0.67)	1.52(0.15)
s	1.06(0.26)	0.90(0.20)	0.66(0.15)	1.28(0.19)	0.45(0.31)	0.37(0.14)	1.11(0.60)
s' (0.01Hz)	0.71(0.04)	0.65(0.08)	0.79(0.05)	0.70(0.05)	0.14(0.01)	0.46(0.03)	0.69(0.02)
s' (1 Hz)	0.49(0.04)	0.47(0.02)	0.62(0.03)	0.62(0.05)	0.13(0.01)	0.28(0.01)	0.48(0.02)
s' (100 Hz)	0.39(0.04)	0.44(0.02)	0.54(0.02)	0.57(0.04)	0.11(0.01)	0.23(0.01)	0.40(0.02)
s' (1 kHz)	0.36(0.04)	0.43(0.03)	0.50(0.02)	0.55(0.04)	0.10(0.01)	0.21(0.01)	0.38(0.02)
s' (1 MHz)	0.23(0.03)	0.33(0.02)	0.42(0.04)	0.46(0.04)	0.07(0.01)	0.18(0.01)	0.31(0.02)
σ_{cf}	$3.80(10^0)$	$6.17(10^0)$	$2.51(10^2)$	$9.12(10^2)$	$2.63(10^{-3})$	$1.07(10^2)$	$1.41(10^2)$
σ_{cb}	$1.00(10^2)$	$1.0(10^2)$	$9.00(10^1)$	$9.00(10^1)$	$4.00(10^{-3})$	$3.33(10^4)$	$1.39(10^5)$
D_s (μm)	12.84	19.13	40.93	13.10	12.34	25.97	28.80
D_m (μm)	7.92	10.89	33.99	9.71	10.00	3.37	15.76
t_m	3.31(0.10)	4.51(0.08)	2.29(0.40)	4.14(0.57)			2.13(0.27)
g_c	1.08(0.02)	1.76(0.01)	0.44(0.03)	0.71(0.10)			0.29(0.06)
$t_m - g_c$	2.23(0.11)	2.75(0.06)	1.85(0.45)	3.43(0.96)			1.84(0.61)

ductivity and the percolation threshold, (b) the dc critical exponents, (c) the volume and frequency dependence of the dielectric constant, (d) dc scaling, (e) magnetoresistance, and (f) ac conductivity and scaling. Table I contains the parameters obtained from the results given and discussed in (a), (b), (c), (d), and (e), Table II the parameters for the Fe_3O_4 system as a function of temperature, and Table III the parameters obtained from ac measurements, given in (f). For comparison, Table IV contains some parameters obtained from previous measurements.

A. dc conductivity and the percolation threshold

The dc conductivity $[\sigma_m(\phi,0)]$ behavior of percolation systems is best illustrated by a plot of the logarithm of the conductivity against the volume fraction (ϕ) of the conducting component, which gives the typical open *S* curve (called the ''sigmoid'' curve by some authors). Figures 1 and 2 show plots for the graphite and Fe_3O_4 systems. Similar plots were done for the other systems and fits to the two-exponent phenomenological equation [Eq. (1)] gave the parameters ϕ_c (or ϕ_{ce}, which denotes the experimental value of ϕ_c in this paper), *t*, and *s*, shown in Table I for all seven cellular systems studied. Results obtained through fitting the dc conductivity results to the combined percolation equations [Eqs. (2) and (3)], with a common ϕ_c, agree with the results given in Table I, within the experimental errors.

The extrapolated conductivity (σ_{cf}) of the conducting components obtained from the above fitting is always found to be lower than the corresponding bulk conductivity (σ_{cb} [obtained from various sources in the literature (Table I)]). This suggests that interparticle contact resistances play a prominent role in determining the conducting properties of the composites, even at the highest volume fractions used in this paper ($\phi \approx 0.25$), a fact we use in our discussion of the results.

It should be noted that the carbon black used in the present study is the same as that used by Heaney[26] in studies of carbon black–polymer composites ($\phi_{ce} = 0.170 \pm 0.001$, $t = 2.9 \pm 0.1$). From the fitting of his experimental data to the percolation equations, Heaney[26] obtained a σ_{cf} for carbon black of 66.7 $(\Omega\ \mathrm{cm})^{-1}$, which is closer to the bulk value of 100 $(\Omega\ \mathrm{cm})^{-1}$ quoted in his paper and is an order of magnitude higher than the values shown in Table I. Note also the significant differences in σ_{cf}, *t*, *s*, and s' (from dielectric constant measurements) and the small difference in ϕ_{ce} for the ground and raw carbon black systems. This implies that the interparticle contacts have been altered by the grinding, which has probably decreased the sharpness of the edges or angularity of the ground carbon black particles. Note that the lower *s* and higher *t* for the raw carbon black system are a little closer to the very angular NbC and Fe_3O_4. The high-*t* NbC and Fe_3O_4 systems, with their hard sharp edges (point contacts), show the largest discrepancies between the extrapolated conductivity and the bulk value (i.e., $\sigma_{cf} \ll \sigma_{cb}$).

The discrepancy between σ_{cf} and σ_{cb} is further illustrated in three graphite-containing systems. In the compacted graphite–boron-nitride system,[7] σ_{cf} was found to be 77.62 $(\Omega\ \mathrm{cm})^{-1}$ compared to 912.01 $(\Omega\ \mathrm{cm})^{-1}$ (obtained from the three-component system of graphite, boron nitride, and talc wax) and 251.00 $(\Omega\ \mathrm{cm})^{-1}$ (obtained from the graphite–talc-wax system). Note that when treating the graphite–boron-nitride coating as an independent, compacted bulk percolation system (see later), σ_{cf} was found to be 44.5

$(\Omega\,\mathrm{cm})^{-1}$, reasonably close to the compacted graphite–boron-nitride system.[7] The differences observed in the σ_{cf} values for these systems seem to indicate that the insulating matrix also affects the value of σ_{cf}. However, in all ''three'' graphite systems discussed above and a previouly measured one,[6,7] the values of the *s* and *t* exponents are fairly close. The values for ϕ_{ce}, *s*, and *t* for some other systems are given in Table IV and discussed later.

The various mechanisms influencing the critical volume fraction (ϕ_c) are now reasonably understood.[2,7] These include the relative sizes of the component particles[27–29] and shape of the particles.[30–33] While all these mechanisms could influence ϕ_{ce} in the composite systems studied in this paper, it appears that the relative size D_i/D_c (where D_i and D_c are the diameters of the insulator and conductor components, respectively) of the two components has the largest effect on the percolation threshold, because of the consistently low ϕ_{ce}'s (<0.065). Therefore, the Kusy model[27] is now experimentally examined in detail, using ''nonideal'' conducting powders. Note that the small conductor particles, embedded on the surface of the large insulating talc-wax particles, form conducting link, blob, and node arrays which, in turn, form the percolation paths or backbones in these 3D systems.

Figure 3 shows the predicted and experimental ϕ_c values superimposed on the Kusy theoretical curve (the numerical results are given in Table I). The experimental values (ϕ_{ce}), which are not functions of D_i/D_c, are given as vertical (dashed) lines and the points where they intersect the theoretical curve are examined. The predicted or calculated ϕ_c values were obtained from the Kusy formula [$\phi_c=1/(1+KB)$, where $B=D_i/D_c$ and K is a constant[27]], using the measured values of the mean size of the particles for each powder from the Malvern size analyzer, and are plotted on the curve. The theoretical points (denoted by subscripts *M* and *S*), shown in Fig. 3 and given in Table I, were obtained by using the ratio of insulator (whose average diameter was measured to be 300 μm) to both the mean (*M*) and Sauter (*S*) diameters of the conductor particles for each system. The Fe_3O_4, ground carbon black, and GBN (15%) system ϕ_{ce} values show good agreement with theory using the mean diameter. The angular, but nearly spherical, Fe_3O_4 and NbC systems show good agreement using the Sauter diameter. In general, the ϕ_c values calculated from the mean and Sauter diameters (ϕ_{cm} and ϕ_{cs}, respectively, in Table I) are always greater than or equal to the experimentally determined critical volume fraction (ϕ_{ce}). The only exception is the niobium carbide system, where the mean diameter value (ϕ_{cm}) is much lower than ϕ_{ce}. The results shown in Fig. 3 and Table I illustrate how the difference for the actual shape from spherical and size distribution of the conductor particles can give rise to the critical volume fraction of the systems, which differ from those predicted on the basis of spherical and monosized particles in the Kusy model. Hence the Kusy model is only a first approximation in estimating ϕ_c in real systems, especially where the particles are not spherical and/or have a wide or abnormal size distribution.

The two carbon black systems show a small difference in the ϕ_{ce} values, which overlap within the error bars. However, the ϕ_{ce} of the ground system is found to be slightly smaller than that obtained in the unground (raw) carbon black system, due to the smaller radius, which would agree with the Kusy model.[27] The plain graphite and graphite mixed with boron nitride (15%) systems also show the same critical volume fraction (within the error limits), which is quite interesting as the latter is essentially a three-component system.

While one may believe that ϕ_{ce} in the cellular systems is primarily dependent on the relative size of the components, a closer examination of the systems shows that there are other important factors involved in determining ϕ_{ce}. Take, for instance, the niobium carbide and graphite systems. From their mean particle sizes (~ 3 μm for NbC and ~ 30 μm for graphite), the niobium carbide should have a lower critical volume fraction than the graphite system (according to the Kusy model) but the reverse is actually true. In fact, the niobium–carbide–talc-wax composite has the highest ϕ_{ce} value of all the systems. It is suggested that the heavy, hard, and angular NbC particles are knocked into the surfaces of the soft talc-wax particles during sample preparation in a way that is likely to reduce the probability of contact between the conductor particles on the talc-wax surface, leading to a higher ϕ_{ce} value. The irregular geometry of the graphite particles, which are in the form of flakes, might also favor a low percolation threshold, as the relatively light graphite flakes lie flat on the talc-wax particles, without penetrating their surfaces, which allows more numerous interparticle contacts than for a similar volume fraction of niobium carbide. The nickel and Fe_3O_4 systems have the same value of ϕ_{ce}, but the reason for such a similar result is not immediately obvious.

The extremely low percolation thresholds of the ground and unground carbon black systems also agree well with previous studies where carbon black particles were blended into polymers.[26,30,34] Connor and his collaborators[34] studied the conductivity of a composite made of highly structured carbon black in an amorphous polymer [polyethylene terephthalate (PET)] and obtained $\phi_{ce}=0.011$, which is in fair agreement with the critical volume fractions obtained for the carbon black systems in this work. The low value of ϕ_{ce} observed in carbon black systems has been attributed to the formation of aggregates by the carbon black particles as noted by Balberg,[30] Heaney,[26] and Connor and co-workers.[34] However, this work indicates that the carbon aggregates probably form a cellular structure coating ''polymer'' grains which contain no or very little carbon.

The only previous experiments directly studying the dependence of ϕ_{ce} on the relative size of the constituent particles of the composite seem to be studies done on RuO_2 (conducting oxide-glass composites), which gave ϕ_{ce} values in the range 0.02–0.04.[28]

B. dc critical exponents

The exponents shown in Table I have a range of values falling close to, below, and above the universally accepted values of *s* and *t*, taken as 0.87 and 2.00, respectively, for 3D percolation systems.[3–5] Four classes of the exponent *t* have

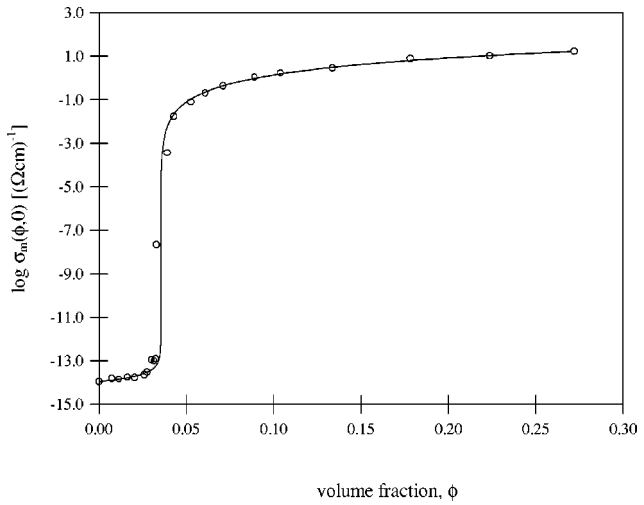

FIG. 1. Plot of the logarithm of dc conductivity $[\sigma_m(\phi,0)]$ results vs the volume fraction (ϕ) of graphite for the graphite system. The solid line is a fit to Eq. (1) and the fitting parameters are $\phi_c=0.035\pm0.002$, $t=1.93\pm0.06$, $s=0.66\pm0.15$, $\sigma_c=251\ (\Omega\ \mathrm{cm})^{-1}$, and $\sigma_i=1.10\times10^{-14}\ (\Omega\ \mathrm{cm})^{-1}$.

been identified from the results in Table I. The first category consists of the nickel system with a t exponent well below the universal value. Unfortunately, there is no explanation or model to account for such a low t value, although values below 2.00 have been previously observed.[12,31]

The second class of t exponents includes the graphite and two carbon black systems, which give t values very close to the universal value of 2.00. Recall that according to Kogut and Straley,[11] systems with a narrow range of conductances should give universal t exponents. It is therefore probable that the carbon and graphite grains form good or reproducible contacts with each other.

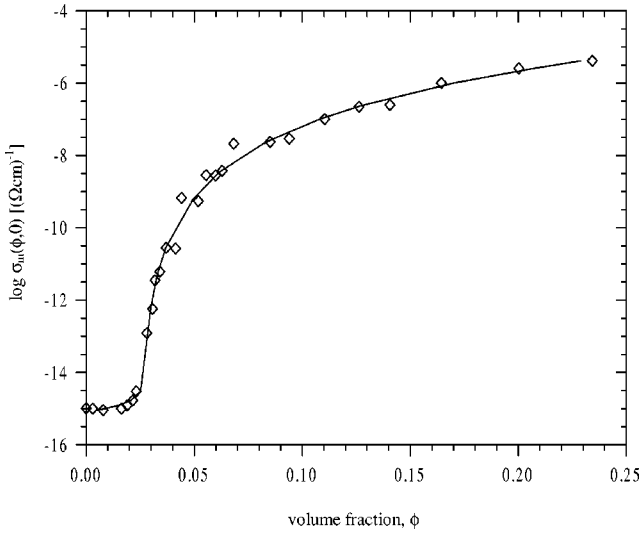

FIG. 2. Plot of the logarithm of dc conductivity $[\sigma_m(\phi,0)]$ results vs the volume fraction (ϕ) of Fe_3O_4 for the Fe_3O_4 system. The solid line is a fit to Eq. (1) and the parameters used in the fitting are $\phi_c=0.025\pm0.003$, $t=4.12\pm0.23$, $s=0.45\pm0.31$, $\sigma_c=2.63\times10^{-3}\ (\Omega\ \mathrm{cm})^{-1}$, and $\sigma_i=8.51\times10^{-16}\ (\Omega\ \mathrm{cm})^{-1}$.

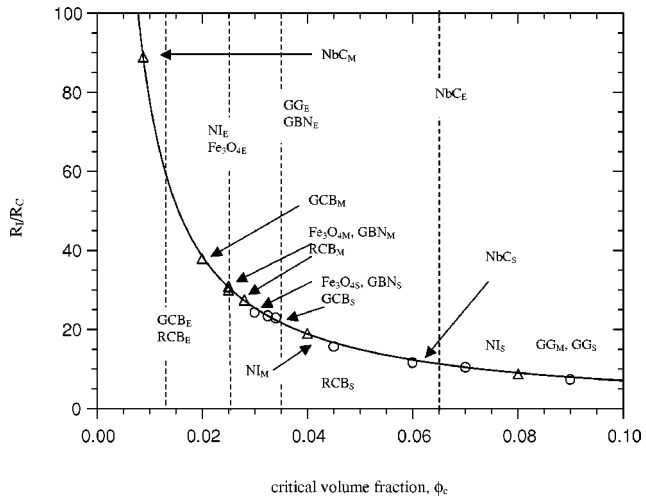

FIG. 3. The Kusy simulation curve with the experimental results superimposed on it: The Kusy theoretical curve (solid line), Experimental (E) values (dotted line), Sauter mean diameter (S) value ($\bigcirc$), and mean diameter (M) value ($\triangle$).

The third class of exponent ($t\sim2.5$) appears only in the graphite–boron-nitride–talc-wax (also referred to as the three-component) system. The reason for especially noting this t exponent is that it agrees well with the upper limit of the original random void model[12–14] of 2.5 or of the new Balberg model,[16] with the $\omega'=0$ case. This confirms that, in some systems, the original random void model can be used as a picture, with the backbone of the percolating conducting powder providing the necks and the insulating particles the large voids. Note that systems involving nickel, carbon black, or graphite have grains which can be assumed to have low and/or a narrow range of contact resistances. Previous results[31,35,36] where the conducting powder was carbon black or graphite all have t values in the range 2.0–2.8.

Previous results which give t values in the range 2.0–2.5 or a little above include those of Deprez and McLachlan[31] who obtained various values of the t exponent in the axial and transverse directions during powder compression experiments involving four different forms of graphite. Values of t for the natural flaky graphite used in these experiments were $(t_{axial}=1.94\pm0.05)$ and $(t_{trans}=2.8\pm0.3)$, with the same ϕ_{ce}. For all four powders, the range of t_{axial} was from 1.5 to 2.7 and t_{trans} from 2.1 to 2.8, indicating the complexity of graphite systems. Chen and Chou[35] obtained $t=2.3\pm0.4$ and $\phi_c=0.0076$ in a carbon-wax mixture (in good agreement with the t value obtained in the raw carbon black system) while Chen and Johnson[36] reported a value of $t=2.2$ and $\phi_c=0.28$ for nodular nickel in polypropylene. Wu and McLachlan[7] obtained t values of 2.63 and 2.68 in the axial and transeverse directions of a series of compressed graphite–boron-nitride pellets ($\phi_c=0.150$). These results, plus others, show that most continuum systems have t values in the range of 2.0–2.5 or even 3.0 and that the t values are not correlated with the critical volume fraction. Recall that the theoretical limit for the RV model is 2.5, and the links node and blob models give 2.35, while the mean field value is 3.0.[26] Note that Lee *et al.*[14] measured a t value of 3.1 in a

random-void-like system (with a presumably continuous indium conducting component), which is well within the range compatible with Eq. (11).

The *t* exponents obtained in the carbon black and graphite cellular composites are well within the range predicted by the theories discussed above and will henceforth be referred to as low-*t* ($t<3$) systems, while those with $t>3$ (discussed below) will be referred to as high-*t* systems.

The last category of *t* exponents was observed in the magnetite (Fe_3O_4) and niobium carbide systems. These composite systems show values of the exponent *t* higher than allowed by the RV model. These high-*t* values of the niobium carbide and magnetite systems are also associated with some of the smallest *s* values ever reported for 3D systems. The extreme values of the *t* exponents can be accommodated by the new Balberg model,[16] which is an extension of the RV model and allows for higher values of the conductivity exponent than any previous theories.

Extreme values of *t* have also been reported in previous experiments. Wu and McLachlan[7] reported values of *t* between 4.80 (axial) and 6.10 (transverse) in very loosely packed graphite–boron-nitride powder composites. Wu and McLachlan attributed the abnormally large *t* values of the powders to the presence of a large number of cavities and microvoids in the samples, where the actual powder mixtures tend to coat the air cavities. Therefore the geometry of this system is similar to the Swiss-cheese or RV model. Note that the contacts between the loosely packed graphite particles are very similar to those between the NbC and Fe_3O_4 particles described here, all of which have a very large range of intergrain resistances. Therefore it would appear that conductors consisting of angular particles lead to high-*t* values and low-*s* values.

While a considerable amount of experimental and theoretical[3–5,7] attention has been focused on the conductivity exponent *t*, very little has been done on the dc exponent *s*. The results presented here were taken over a wide range of ϕ values, below and above ϕ_c, which enabled the simultaneous determination of the exponents *t* and *s* as well as ϕ_{ce}, σ_c, and σ_i. Values of *s* given in Table I range from 0.37 to 1.28, with the upper limit given by the three-component system of graphite, boron nitride, and talc wax. As mentioned earlier, the NbC and Fe_3O_4 systems are among the systems with the smallest *s* values ever reported in 3D continuum systems. Values in the range 0.65–1.00, reasonably close to $s_{un}=0.87$, are obtained in the GG, GCB, and RCB systems, whose *t* values are also reasonably close to the universal value ($t_{un}=2.00$).

To the best knowledge of the authors, no previous experiments, in continuum systems, have reported measurements of the exponent *s* from conductivity measurements other than the work reported in Ref. 7. Reference 7 reported a value of $s=1.01\pm0.05$ in graphite–boron-nitride disk samples and extremely low values of *s* in 50% graphite–50% boron-nitride (0.42 ± 0.01) and 55% graphite–45% boron-nitride (0.47 ± 0.01) powder systems. The latter two values were obtained from measurements done in the axial (pressure) direction. Note again that low-*s* (and -s') values are associated with high *t* values. No simple qualitative correlation between *s* and *t* (eg $t/s=$const) was found.

C. Volume and frequency dependence of the dielectric constant

In this study, dielectric measurements were made on the samples used in the dc conductivity experiments, in the frequency range of 10^{-2}–10^{6} Hz, as a function of ω, for $\phi<\phi_{ce}$. The s' values were obtained from the best linear fits to the graph of $\log[\epsilon_{mr}(\phi,\omega)/\epsilon_{mr}(0,\omega)]$ [the real part of the dielectric constant, normalized by the dielectric constant of the insulator ($\phi=0$ sample)] against $\log(\phi_{ce}-\phi)$, where ϕ_{ce} is the critical volume fraction of the conductor, obtained from the dc measurements. Results for all systems are shown in Table I, where it can be clearly seen that s' is frequency dependent, increasing towards its dc or zero-frequency value (*s*) as the frequency is lowered. Note that 1000 Hz is the frequency used in most previous dielectric measurements. Note also that from standard percolation theory, one would expect that the s' values at the various frequencies would all be the same. The results shown in Table I indicate that the exponent *s* is usually larger than s'. Note that the largest change in s' with frequency is for Fe_3O_4. However, as NbC shows changes similar to the other samples, the changes in s' may not be solely associated with a very angular granular conducting phase. As these are the only results for s' as a function of frequency ever to be published, it is not possible to compare them with previous results.

The results given in Refs. 8 and 9 show that the experimental dielectric constants, below ϕ_c, are frequency dependent, in agreement with Eq. (1). As the main thrust of Refs. 8 and 9 was concerned with the dielectric hump above ϕ_c, further model simulations were carried out to examine the dielectric behavior below ϕ_c. These simulations confirm the frequency dependence of s' for systems where $\epsilon_0\epsilon_r/\sigma_c$ is finite and that for $\epsilon_0\epsilon_r/\sigma_c$ tending to zero the dielectric constant becomes frequency independent and diverges on both sides of ϕ_c, in accordance with the predictions given in Refs. 3–5.

Percolation theory as given by various authors[3–5,18] and reviewed in Refs. 3–5 requires that $s=s'$. However, the present results confirm previous results of Wu and McLachlan,[7] who showed that the *s* obtained from dc measurements and the s' (obtained from dielectric measurements) are not the same. Wu and McLachlan measured *s* (from dc conductivity measurements) and s' (at 100 Hz and 1 kHz) in the three graphite–boron-Nitride systems described earlier. The results at 1 kHz are 0.53 for the compacted disks in the axial direction and 0.60(0.72) and 0.91(0.83) for the powders, with 50%(55%) graphite, in the axial and transverse directions, respectively. Note that the two graphite–boron-nitride powder systems are the only ones so far measured with s' clearly larger than *s*. Other experiments that have actually measured the exponent s' have always implied that it was the same as the dc exponents.[36,37]

D. dc scaling

In this paper dc scaling, for different σ_i/σ_c values, has been done using a real composite system. It was intended that the ratio (σ_i/σ_c) would decrease due to the increase of the conductivity (σ_c) of the Fe_3O_4 with temperature. However, in the Fe_3O_4-talc-wax composite, it was observed that σ_i of the talc wax increased appreciably faster with temperature than σ_c of the Fe_3O_4, which resulted in a net increase (rather than a decrease) in σ_i/σ_c with temperature, as shown in Table II. Note that all samples for this system were annealed at 140 °C for 12 h prior to the measurements. This means that the relative thermal expansions were similar and/or any differential expansion was taken up in the soft wax.

The values of s, t, σ_i, and σ_c, shown in Table II, were obtained from fitting the dc conductivity data (at different temperatures) to Eq. (1). Unfortunately, due to the changes in both σ_i and σ_c, the ratio (σ_i/σ_c) changed by only two orders of magnitude in the temperature range from 298 K (25 °C) to 393 K (120 °C). However, this change in (σ_i/σ_c) was still sufficient to move the experimental points along the scaling curve, generated by Eq. (1), as shown in Fig. 4. The values of σ_i and σ_c were obtained as the best fit parameters, which also yielded new values of *t but not* ϕ_c (Table II). Note that values of σ_i close to $\phi=0.00$ could not always be accurately measured, which made it impossible to obtain reliable values of the exponent s or to scale the results below ϕ_c. The values of the parameters, given in Table II, were used to both scale the experimental results and obtain the theoretical curves. The small variations in the exponent t, observed at each temperature, gave rise to slightly different theoretical curves above $x_+=1$ (the solid lines in Fig. 4) onto which the experimental results were scaled. These differences are smaller than the experimental errors. The theoretical curves below ϕ_c are shown merely for the reader's benefit, as reliable data could not be taken in this region. The scaling of the experimental points shown on the graph can be seen through their movement along the curves as the temperature increases from 298 to 393 K. Note the fact that the experimental points at different temperatures all lie on nearly the same curve. It is also interesting to observe that points in the region $\log\{(\sigma_i/\sigma_c)[(1-\phi_c)^{t+s}/(\phi-\phi_c)^{t+s}]\}<2$, slide smoothly along the curve. This illustrates the fact that Eq. (1) can be used to generate valid continuous dc as well as ac (Ref. 6 and this paper) scaling functions. Standard percolation theory does not give a scaling expression in the region $\log x_+$ and $\log x_-\approx 1$. Actually, it only predicts the slopes for x_+ and x_- much less than and much greater than 1. Note that no new experimental parameters, such as the ω_{c+} and ω_{c-} used later in ac scaling, are necessary to enable the dc experimental points to be fitted onto a single scaling curve.

E. Magnetoresistance

In all the systems measured in this study, the change in resistance with magnetic field (magnetoresistance) obeys the expected H^2 (where H is the magnetic field) dependence with reasonable accuracy. The graphite systems and those previously measured show a positive magnetoresistance, while those containing carbon black show a negative magnetoresistance. The reason for the negative magnetoresistance in the two carbon black systems is unclear at this stage. Figures 5 and 6 show the combined plots of the relative magnetoresistance and the magnetoconductivity results, respectively, for the ground carbon black and graphite systems, from which the exponents g_c and t_m were obtained. Note that in the case of the carbon black systems (which show negative magnetoresistance), absolute values are plotted on the y axis. Table I shows the values of t_m and g_c [Eqs. (12) and (13)] for all systems measured. Previous workers[7,25] obtained a g_c value around 0.30, prompting speculations that g_c might be universal. Although some systems from the present study have g_c values close to 0.30, it is clear that the value of g_c is not universal, as most of the systems give a g_c considerably higher than 0.30. Note that the magnetoconductivity exponent (t_m) for all the systems is always greater than the exponent t obtained from dc conductivity measurements, in agreement with previous results.[7,25] Also included in Table I are the values of t_m-g_c, which, as expected, are close (i.e., within the experimental errors) to the experimentally determined values of t. This result is in agreement with that obtained on graphite–boron-nitride disk samples.[7]

F. ac conductivity and scaling

This subsection reports on the ac conductivity studies made on all but the nickel system, which was too conducting to give results in the x_+ or $x_-\geqslant 1$ regime and are not presented. All the parameters and exponents obtained from ac measurements and some important dc ones are listed in Table III. Some of the parameters in Table III are defined later in this section. As this subsection covers a number of topics it has been divided into *ac conductivity results, ac scaling and critical exponents, properties of the critical frequencies, the loss angle*, and *other topics*.

The ac conductivity results. The ac conductivity results for two representative systems (graphite–boron-nitride and niobium carbide systems) are shown in Figs. 7 and 8, where the real part $[\sigma_{mr}(\phi,\omega)]$ of the complex conductivity $[\sigma_m(\phi,\omega)]$ is plotted as a function of frequency. These results show clearly the difference in behavior between the insulating and conducting samples. Samples above the percolation threshold show a frequency-independent behavior at low frequency. As the frequency of the applied signal is increased above a certain value ω_c, referred to here as the crossover frequency, the conductivity starts to increase (from its constant dc value) due to the extra contribution from the capacitive regions, which offer ever-decreasing impedance to the current flow. There is also a tendency for the results in some systems (NbC and Fe_3O_4) to show an as-yet inexplicable upward hook at high frequencies. Figure 8 shows this phenomenon in the NbC system, but the effect is even more pronounced in the Fe_3O_4 system. It is not clear whether the high-t exponents (which are 4.12 ± 0.23 for the Fe_3O_4 and 5.25 ± 0.67 for the NbC system) of the systems have anything to do with the ''hooks.'' Heaney also observed the upward hooks in a carbon-black–polyethylene system, with $t=2.9\pm0.1$.[26]

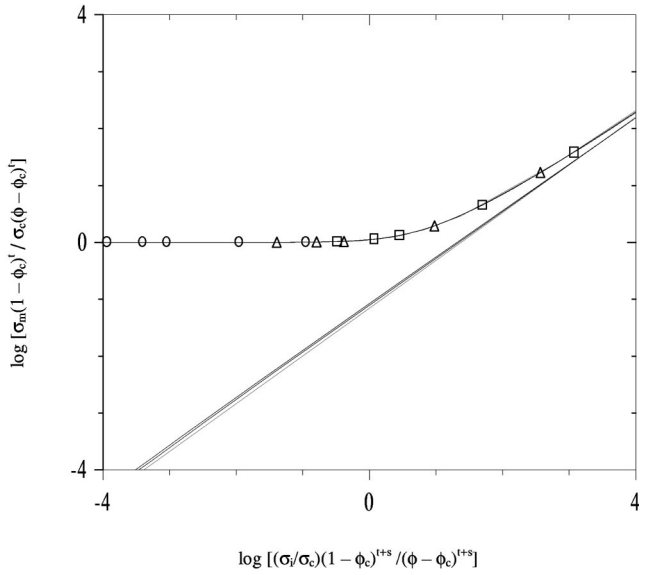

FIG. 4. dc scaling in a magnetite (Fe_3O_4)-talc-wax composite system for samples close to but above ϕ_c at three temperatures 25 °C (○), 80°C (△), and 120°C (□). Note that σ_m on the *y* axis is either the experimental value or the one generated by Eq. (1) at the different temperatures (represented by the dashed and solid lines).

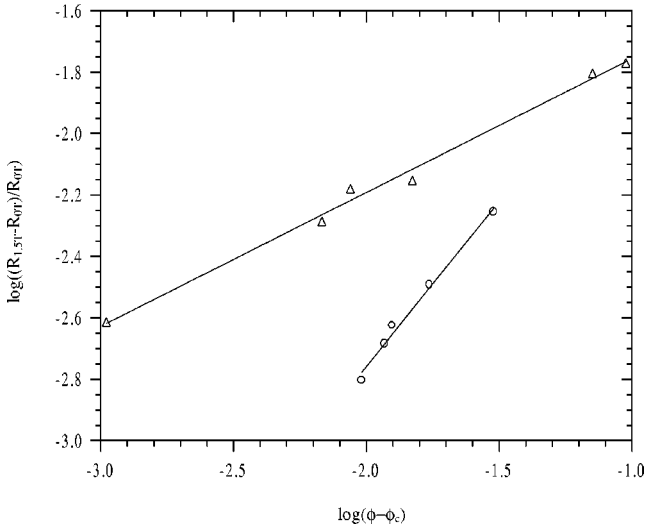

FIG. 5. Log-log plot of the relative magnetoresistance against $(\phi-\phi_c)$ for the ground carbon black (○) and graphite systems (△). The solid lines are a linear fit to the data, which yields $g_c = 1.08 \pm 0.02$ for the carbon black system and $g_c = 0.44 \pm 0.03$ for the graphite system.

The slopes of the conductivity curves for the samples below ϕ_c (Figs. 7 and 8) can be explained as follows. Below ϕ_c, there are two dielectric loss terms contributing to ε_{mi}. For zero and low ϕ the dominant contribution is due to the talc-wax insulator (ε_{ir}) and for larger ϕ the contribution from the conducting clusters ($\sigma_{mr}/\varepsilon_0\omega$) should become visible in the Figs. 7 and 8.

Figures 7 and 8 show that the conductivity curves level off at low frequencies, indicating a small but finite dc conductivity. As all necessary precautions were taken to avoid moisture contamination of the samples (by storing both the powders and compressed samples in dessicators with silica gel), this finite conductivity is almost certainly not due to moisture. Therefore, as it is also present in the $\phi = 0.00$ sample, the finite dc conductivity must be a fundamental property of the insulating component.

For low-ϕ samples, in the frequency range $1-10^5$ Hz, the dielectric loss term of the insulator (with a slope of ~ 0.90), as observed in most dielectric systems, is dominant. From about 10^5 to just over 10^8 Hz, the slope drops below 0.90 before it starts to increase again. Below 10^5 Hz, the dielectric loss term appears to be just a scaled-up talc-wax loss term, which is due to the conducting clusters enhancing the dielectric constant of the insulating components, both real and imaginary. In this region no effects due to the conducting component can be identified. However, as the frequency increases above 10^5 Hz, the insulator has a slope considerably lower than 0.90 (curve *a* in Fig. 7). This allows the loss due to the conducting clusters to be clearly visible above 10^7 Hz (curve *b* in Fig. 7) for the graphite–boron nitride system. Unfortunately, no quantitative information about the percolation loss can be obtained from this or any other system. However, for ϕ close to ϕ_c and at high frequency, the slopes are similar (as expected from theory) to those for the samples above ϕ_c. Previous results in this region, for a G-BN powder system, which has a very low ε_{ir}, have been modeled with reasonable success,[8] using Eq. (1).

ac scaling and critical exponents (u and v): *results and parameters*. Shown in Figs. 9 and 10 are the scaled results for the raw carbon black and niobium carbide systems, using the normalizations described in Sec. II. The value of ω_{c+} for each sample was determined from the point where the backward projection of the high-frequency conductivity curve,

TABLE II. Percolation parameters from the Fe_3O_4 system as a function of temperature. N.B. The fitted $\phi_c(\phi_{ce})$ was always between 0.025 ± 0.003 and 0.025 ± 0.004 across the temperature range. The results below ϕ_{ce} were rather noisy, hence the large statistical errors in *s*.

$T(K)$	$\sigma_c(\Omega\ \mathrm{cm})^{-1}$	$\sigma_i(\Omega\ \mathrm{cm})^{-1}$	σ_i/σ_c	s	t
298	3.219×10^{-3}	3.472×10^{-17}	1.079×10^{-14}	1.01 ± 0.88	4.24 ± 0.28
333	4.939×10^{-3}	5.458×10^{-15}	1.105×10^{-12}	0.86 ± 0.62	3.91 ± 0.22
353	7.998×10^{-3}	1.711×10^{-12}	2.140×10^{-12}	1.15 ± 2.21	3.90 ± 0.25
373	1.050×10^{-2}	1.615×10^{-13}	1.591×10^{-11}	0.80 ± 1.27	3.76 ± 0.21
393	1.419×10^{-2}	1.105×10^{-12}	7.784×10^{-11}	0.80 ± 1.05	3.71 ± 0.21

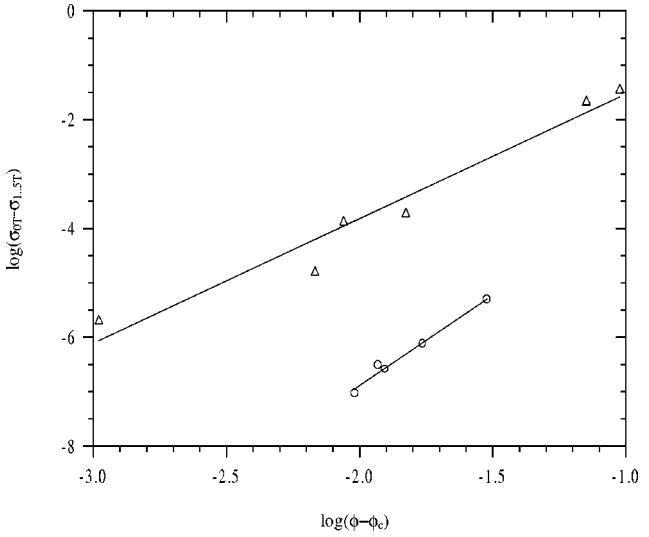

FIG. 6. Log-log plot of the magnetoconductivity against $(\phi - \phi_c)$ for the ground carbon black (○) and graphite systems (△). The solid lines are a linear fit to the data, which yields $t_m = 3.31 \pm 0.10$ for the carbon black system and $t_m = 2.29 \pm 0.40$ for the graphite system.

after it had been divided by $\sigma_m(\phi,0)$, intersected the $\log[\sigma_{mr}(\phi,\ \omega)/\sigma_m(\phi,0)] = 0$ line. These values of ω_{c+} $(1/\omega_{c+})$ were then used to scale the conductivity results of each sample along the log ω axis, or now the ω/ω_{c+} axis, until they coincided. The scaling exponent (u) was obtained from a linear fit to the regions of the scaled plots where $\log(\omega/\omega_{c+}) > 1$. Table III gives the experimental values of u (denoted u_e) for all the systems studied. The intercluster polarization model[3,4,18] predicts that $u = t/(s+t)$. Using the s and t given in Table III, a theoretical exponent (u_t) can be calculated from the above expression and the values are also given in Table III. For comparison, u_t' values, obtained when s is replaced by s' (as determined from dielectric measurements at 1 kHz), are also included and are always found to be closer to u_e than u_t. Note that because of the decrease in s' with frequency in the cellular systems, the values of u_t' at 1 MHz are always found to be greater than those calculated using s' (1 kHz) and, hence, show more disagreement with u_e values than the 1 kHz results.

As noted earlier, scaling laws require that the scaled experimental results of the complex ac conductivity on the conducting side of the percolation threshold $(\phi > \phi_c)$ depend only on ω/ω_{c+}. To test this, Figs. 9 and 10 show not only the experimental results for the raw carbon black and niobium carbide systems, respectively, but also the theoretical curves for $\mathrm{Re}\,F_+$ and $\mathrm{Re}\,F_-$. The curves were calculated from the fitted dc conductivity parameters of σ_c, σ_i, ϕ_c, s, and t using Eqs. (1), (5), (6), (7), and (8). The F_+ curve obtained using s' (1 kHz) and denoted F_+' is also included for comparison.

The results shown in Fig. 9 and for the other low-t $(t < 3)$ systems have some common features. According to theory, the curves (F_+) should have a slope of $u = t/(s+t)$ for $(\omega/\omega_{c+}) > 1$ and the experimental results are expected to lie on these curves. The scaled experimental results obtained from the low-t $(t < 3)$ cellular systems do lie near the F_+ theoretical curves, as can be seen in the above figures and Table III. However, the experimental results are found to lie closer to the F_+' curves [with slopes given by $t/(s'+t)$] than

TABLE III. Experimental ac parameters measured in this paper. GCB, ground carbon black; GG, ground graphite; Fe_3O_4, Magnetite; RCB, raw carbon black; GBN, graphite/boron nitride; NbC, niobium carbide.

	GCB	RCB	GG	GBN	Fe_3O_4	NbC
ϕ_c	0.0122±0.0007	0.0131±0.0006	0.035±0.002	0.033±0.001	0.025±0.003	0.065±0.003
s	1.06±0.26	0.90±0.20	0.66±0.15	1.28±0.19	0.45±0.31	0.37±0.14
s'	0.36±0.04	0.43±0.03	0.50±0.02	0.55±0.04	0.10±0.01	0.21±0.01
t	2.06±0.10	2.26±0.11	1.93±0.06	2.51±0.12	4.12±0.23	5.25±0.67
u_e	0.78±0.01	0.85±0.01	0.84±0.01	0.77±0.01	0.73±0.01	0.71±0.01
u_t	0.66±0.19	0.72±0.20	0.74±0.19	0.66±0.13	0.90±0.67	0.93±0.47
u_t'	0.85±0.14	0.84±0.10	0.79±0.06	0.82±0.10	0.98±0.15	0.96±0.17
v_e	0.119±0.004	0.074±0.003	0.106±0.004	0.059±0.002	0.051±0.003	0.042±0.002
v_t	0.34±0.10	0.28±0.08	0.25±0.06	0.34±0.07	0.10±0.07	0.07±0.04
v_t'	0.15±0.02	0.16±0.02	0.21±0.01	0.18±0.02	0.020±0.003	0.040±0.007
u_e+v_e	0.90±0.01	0.92±0.01	0.95±0.01	0.83±0.01	0.78±0.01	0.75±0.01
q_e	1.47±0.09	1.40±0.03	0.84±0.01	0.96±0.05	1.06±0.04	1.67±0.13
q_t	1.51±0.44	1.40±0.38	1.34±0.35	1.51±0.30	1.11±0.82	1.07±0.54
q_t'	1.17±0.19	1.19±0.14	1.26±0.09	1.22±0.15	1.03±0.16	1.04±0.18
z	0.92±0.01	0.91±0.02	0.92±0.01	0.90±0.01	0.85±0.02	0.79±0.01
δ_{ce}	5.09±0.15	3.61±0.12	3.45±0.10	4.75±0.10	0.29±0.05	1.14±0.05
δ_{ct}	0.53±0.16	0.45±0.12	0.40±0.10	0.53±0.10	0.16±0.12	0.10±0.05
δ_{ct}'	0.23±0.04	0.25±0.07	0.32±0.08	0.28±0.05	0.04±0.03	0.06±0.03
δ_{cu}	0.345±0.004	0.236±0.003	0.251±0.003	0.361±0.005	0.424±0.006	0.456±0.006
δ_{cv}	0.187±0.006	0.116±0.004	0.116±0.006	0.093±0.005	0.080±0.005	0.066±0.003

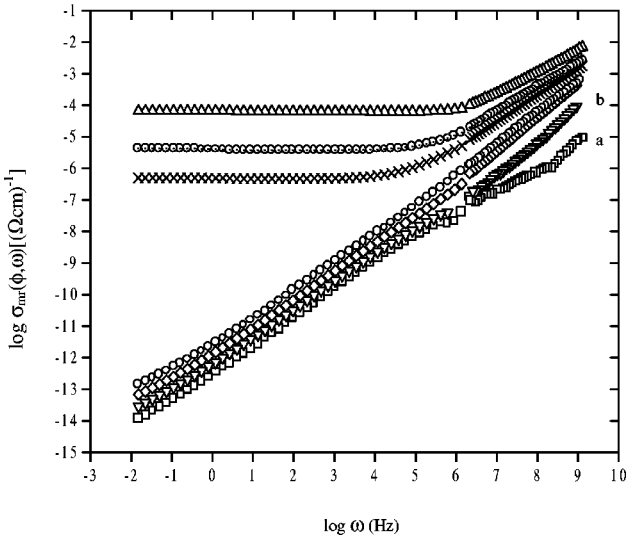

FIG. 7. A log-log plot of ac conductivity vs frequency for the graphite–boron-nitride system over the full experimental frequency range used. [$\phi=0.0000$ ($\square$), $\phi=0.0169$ (∇), $\phi=0.0270$ ($\diamond$), $\phi=0.0333$ ($\times$), $\phi=0.0336$ ($\odot$), $\phi=0.0345$ (Δ), with $\phi_c=0.033\pm0.001$]. The samples $\phi=0.0167$, 0.0176, 0.0299, and 0.0351 have been left out in order to avoid congestion.

the F_+ curves. This shows that s' (1 kHz) is usually in better agreement with scaling theory than the exponent s. This observation underscores the need to measure both s and s' in percolation systems. The high-t systems of NbC and Fe_3O_4 belong to a different category, as the scaled experimental results lie further away from either the F_+ or F'_+ curves (refer to Fig. 10) than the low-t systems. This is immediately

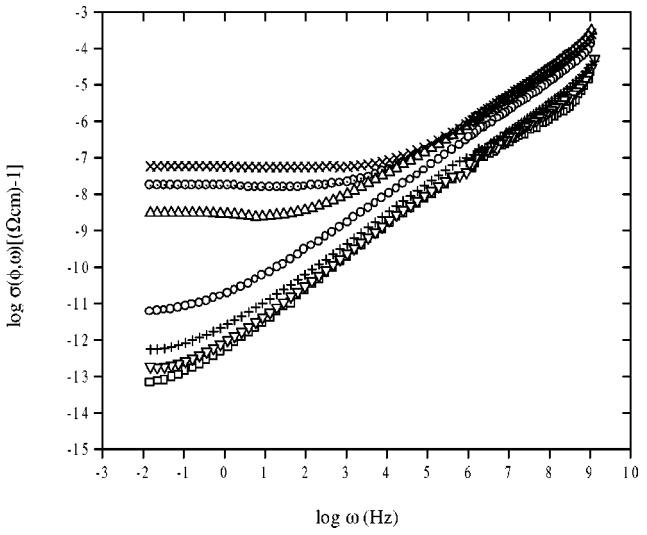

FIG. 8. A log-log plot of ac conductivity vs frequency for the niobium carbide system over the full frequency range. [$\phi=0.0000$ ($\square$), $\phi=0.0080$ (∇), $\phi=0.0653$ ($+$), $\phi=0.0742$ ($\bigcirc$), $\phi=0.0799$ (Δ), $\phi=0.0831$ ($\odot$), $\phi=0.0874$ ($\times$), with $\phi_c=0.065\pm0.006$]. Notice the upward hooks in the data at high frequency for this system. The samples $\phi=0.0187$, 0.0210, 0.0329, 0.0485, 0.0610, 0.0670, 0.0714, and 0.0733 have been left out in order to avoid congestion.

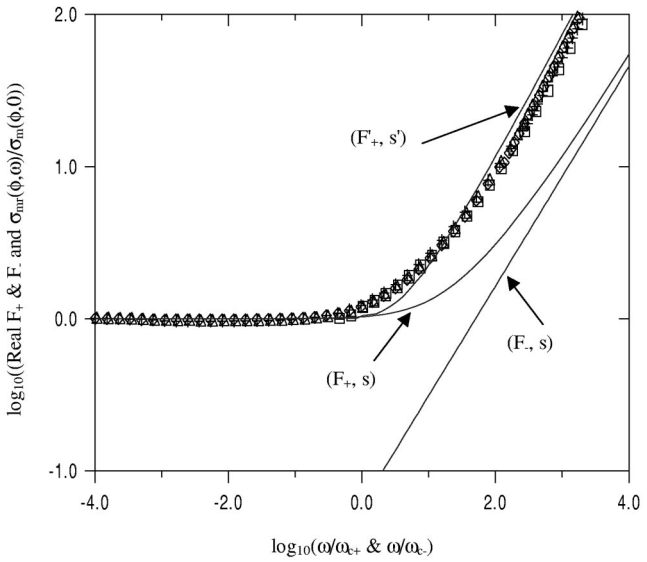

FIG. 9. A log-log plot of the reduced ac conductivity vs reduced frequency for the raw carbon black system for the samples $\phi=0.01291$ ($\square$), $\phi=0.01343$ (Δ), $\phi=0.01351$ ($\diamond$), and $\phi=0.01334$ ($+$). The scaling functions F_+ and F_- (solid lines) are obtained using the dc parameters $\sigma_c=6.166$ $(\Omega\ \mathrm{cm})^{-1}$, $\sigma_i=\omega 8.84\times10^{-13}$ $(\Omega\ \mathrm{cm})^{-1}$, $\phi_c=0.0131\pm0.0006$, $s=0.90\pm0.20$, and $t=2.26\pm0.11$. F'_+ is obtained using the same parameters but with s replaced by $s'=0.43\pm0.03$. Note the close agreement between F'_+ and the experimental results.

obvious from Table III, where the values of u_e, u_t, and u'_t for the high-t systems are very different.

Below ϕ_c, the exponent v is obtained from the log-log plot of the imaginary part of the ac conductivity $[\omega\varepsilon_{mr}(\phi,\omega)]$ against frequency using the relationship $\omega\varepsilon_{mr}(\phi,\omega)\propto\omega^{1-v}$. Alternatively, the exponent v can be obtained from the log-log plot of the real dielectric constant against frequency using the relation $\varepsilon_{mr}(\phi,\omega)\propto\omega^{-v}$. Some representative plots based on this relation are given in Figs. 11 and 12, which show the results for the raw carbon black and niobium carbide systems, respectively. The values of v for all the systems range from 0.04 to 0.12, with the lowest values being obtained from the high-t and low-s systems, containing Fe_3O_4 and NbC powders. These experimental values are all lower than values obtained from calculations, based on the intercluster polarization model.[3,18] The model also predicts that u and v should satisfy the relation $u+v=1$. Using the experimental values of u and v in Table III, only the ground graphite, ground carbon black, and raw carbon black have values reasonably close to unity. Note that these systems have s and t values (Table I) close to the universal values. The rest of the systems have their sum of u_e and v_e exponents well below unity, even when the errors are taken into account. The u_e+v_e results in Table III also show a strong tendency to decrease as the t exponent increases. This may be a unique characteristic of the cellular systems.

Properties of the critical frequencies. The critical frequencies ω_{c+} and ω_{c-} display certain properties, according to the equations given in Sec. II. The first of these is that the fre-

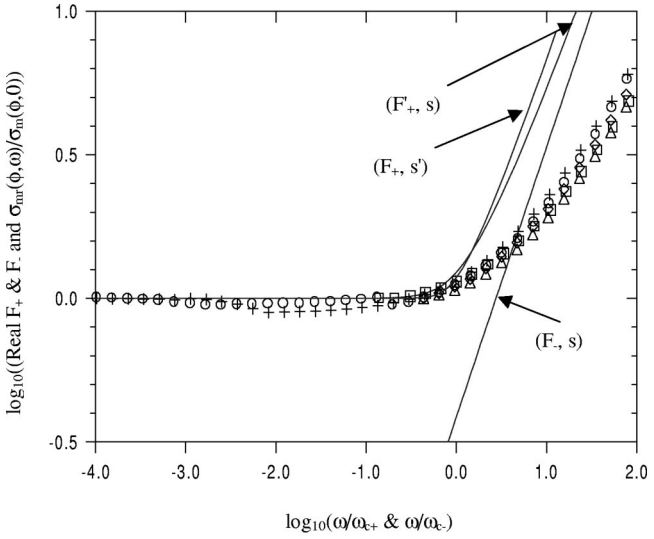

FIG. 10. A log-log plot of the reduced ac conductivity vs reduced frequency for the niobium carbide system for the samples $\phi=0.0714$ (∇), $\phi=0.0733$ ($\square$), $\phi=0.0742$ ($\diamond$), $\phi=0.0831$ ($+$), and $\phi=0.0874$ ($\bigcirc$). The scaling functions F_+ and F_- (solid lines) are obtained using the best-fit dc parameters $\sigma_c=107.2\ (\Omega\ \mathrm{cm})^{-1}$, $\sigma_i=\omega 8.84\times10^{-13}\ (\Omega\ \mathrm{cm})^{-1}$, $\phi_c=0.065\pm0.006$, $s=0.37\pm0.14$, and $t=5.25\pm0.67$. F'_+ is obtained using the same parameters but with s replaced by $s'=0.21\pm0.01$. Note the disagreement between both F_+, F'_+ and the experimental results.

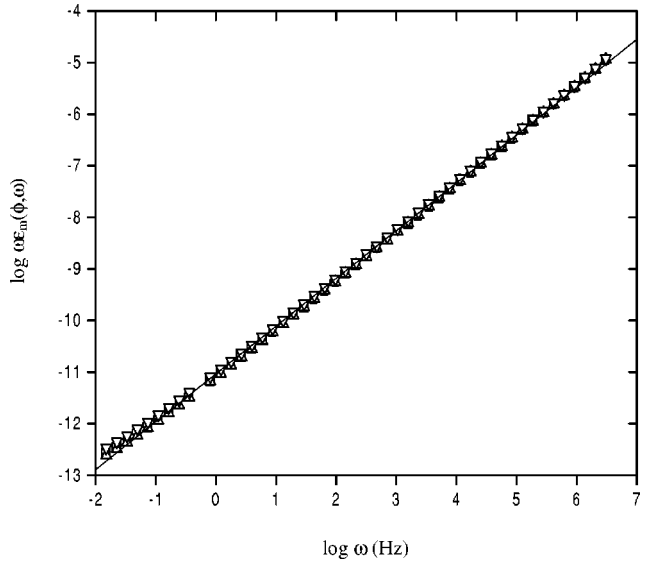

FIG. 11. A log-log plot of the imaginary ac conductivity $[\omega\varepsilon_m(\phi,\omega)]$ against the frequency (ω) for the raw carbon black system. The solid line is a linear fit to the data from which the value of the exponent v_e [from $\omega\varepsilon_m(\phi,\omega)\propto\omega^{1-v_e}$] is found to be $v_e=0.074\pm0.003$ [$\phi=0.01044$ ($\square$), $\phi=0.01088$ ($\bigcirc$), $\phi=0.01077$ (Δ), $\phi=0.01134$ (∇), with $\phi_c=0.0131\pm0.0006$].

quency ω_{c+} should scale with the dc conductivity as $\omega_{c+}\propto\sigma_m(\phi,0)^q$,[6,38] where q is an exponent whose experimental value is denoted q_e in this paper. Figures 13 and 14 show log-log plots of the experimental values of ω_{c+} against $\sigma_m(\phi,0)$ for the graphite and Fe_3O_4 systems respectively. Table III gives the experimental values of q_e for all the systems studied. The intercluster polarization model gives the exponent q or q_t in terms of the conductivity exponent t and the dielectric exponents s and s' as $q_t=(s+t)/t$ and $q'_t=(s'+t)/t$, which show that q_t and q'_t should never be less than unity. Values of q_t and q'_t were calculated using the dc s and t and t with s' (1 kHz), respectively. The results are shown in Table III.

The experimental values of q (q_e) for the cellular systems can be sorted into two categories: q_e greater and less than unity. The $q_e>1$ category includes the two carbon black systems, whose q_t and q_e values are also in very good agreement. Systems with $q_e<1$, in conflict with theory, include the two graphite systems and the three-component (graphite–boron-nitride–talc-wax) system.

The high-t systems of Fe_3O_4 and NbC also give q_e values greater than unity, with the NbC system having the largest value of q_e. The other high-t system (Fe_3O_4–talc-wax system) has a lower q_e value which is in good agreement with the intercluster model for both s and s'. In addition, only the niobium carbide system gives $q_e>q_t$, which seems to indicate that this high-t system is itself unique.

Values of ω_{c+} can also be calculated using $\omega_{ct}=(\sigma_c/2\pi\varepsilon_0\varepsilon_{ri})|\phi-\phi_c|^{t+s}$ and the dc experimental values of σ_c, ϕ_c, s, and t. Since the relative dielectric constant (ε_{ri}) of the insulator or talc wax is frequency dependent, an

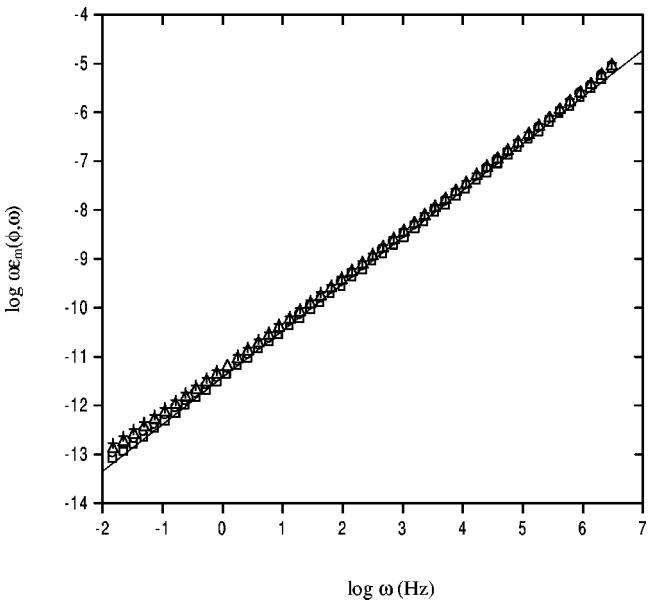

FIG. 12. A log-log plot of imaginary ac conductivity $[\omega\varepsilon_m(\phi,\omega)]$ against the frequency (ω) for the niobium carbide system. The solid line is a linear fit to the data from which the value of the exponent v_e [from $\omega\varepsilon_m(\phi,\omega)\propto\omega^{1-v_e}$] is found' to be $v_e=0.042\pm0.002$ [$\phi=0.0329$ ($\square$), $\phi=0.0610$ ($\bigcirc$), $\phi=0.06528$ (Δ), $\phi=0.06705$ ($+$), with $\phi_c=0.065\pm0.006$].

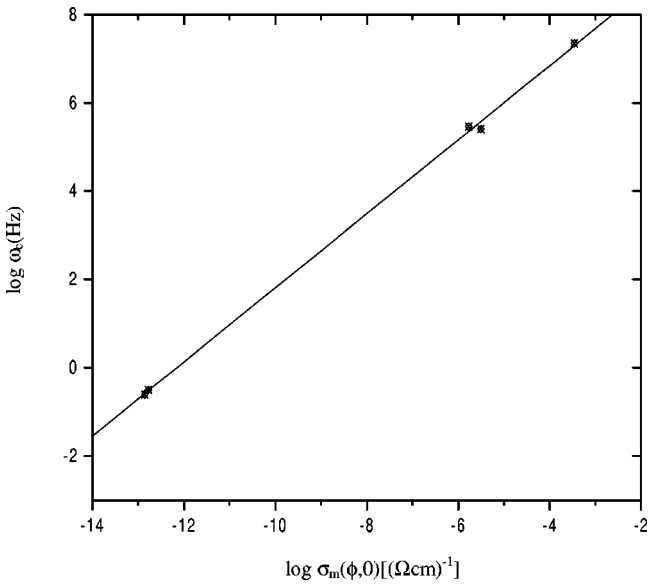

FIG. 13. A log-log plot of ω_c against dc conductivity $[\sigma_m(\phi,0)]$ for the graphite system. The solid line is a linear fit to the data from which the value of the exponent q_e [from $\omega_{c+} \propto \sigma_m(\phi,0)_e^q$] is found to be $q_e = 0.84 \pm 0.01$.

average value of 7.00 was assumed for ε_{ri} in the frequency range 10^0–10^6 Hz, where most of the experimental ω_{c+} (denoted ω_{ce}) values lie. It is observed that systems with low-*t* exponents have $\omega_{ce} > \omega_{ct}$ [e.g., for the raw carbon black system, $\omega_{ce}(\omega_{ct})$ are 1.995×10^4 (3.300×10^2), 5.012×10^4 (1.043×10^3), and 6.310×10^5 (1.892×10^4), for increasing ϕ] whereas the opposite ($\omega_{ce} < \omega_{ct}$) is true for the high-*t* systems [e.g., for the Fe_3O_4 system, $\omega_{ce}(\omega_{ct})$ values are 1.000×10^2 (1.640×10^2), $7.244\times10^2(1.034\times10^3)$, 1.000×10^4 (9.573×10^3), and 1.000×10^5 (1.296×10^5)]. No model exists for this behavior. It is also worth noting that the calculated and experimental values of ω_{c+} for the high-*t* Fe_3O_4 system are reasonably close in comparison with other systems studied in this paper. Note that the graphite–boron-nitride disk system[6] also gave $\omega_{ce} \approx \omega_{ct}$, while for the powder systems,[6] ω_{ce} was at least two orders of magnitude greater than ω_{ct}.

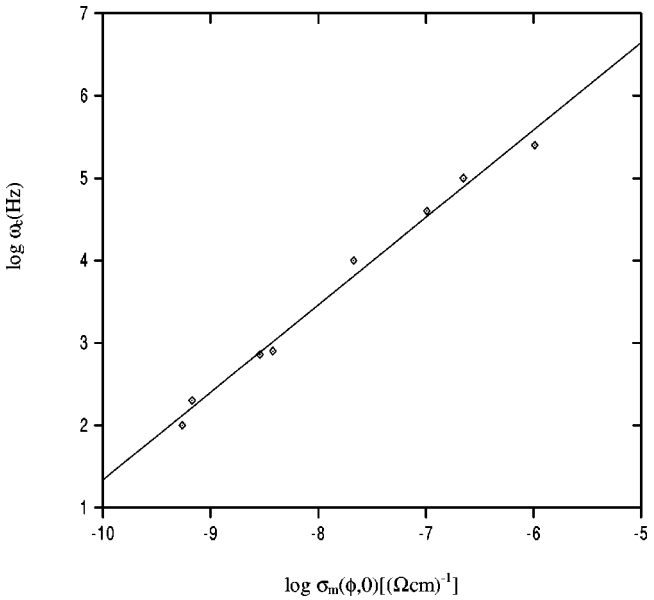

FIG. 14. A log-log plot of ω_c against dc conductivity $[\sigma_m(\phi,0)]$ for the Fe_3O_4 system. The solid line is a linear fit to the data from which the value of the exponent q_e [from $\omega_{c+} \propto \sigma_m(\phi,0)_e^q$] is found to be $q_e = 1.06 \pm 0.04$.

The loss angle (δ). For a material with complex ac conductivity, the loss angle (δ) is given by the relation $\tan\delta = \sigma_{mr}(\phi,\omega)/\omega\varepsilon_{mr}(\phi,\omega)$. Figures 15 and 16 show log-log plots of the loss tangent ($\tan\delta$) versus frequency for the raw carbon black and Fe_3O_4 systems, very close to the percolation threshold. Similar results are observed for all six systems. Numerical simulations using Bruggeman symetric media theory, done on the conducting side of the percolation threshold,[3] give the same qualitative result. In the present systems for ϕ below ϕ_c, $\tan\delta$ is less frequency dependent, in agreement with intercluster polarization predictions.[3] The high-*t* systems show a minimum in $\tan\delta$ between 10^8 and 10^9 Hz, after which the curves show upward hooks, similar to those observed in the ac conductivity plots in the same frequency range. There is no available explanation for this result.

Above ϕ_c, $\tan\delta$ is highly frequency dependent for all systems and is expected to obey $\tan\delta \propto \omega^{-z}$ at low frequencies. From their measurements, Chen and Johnson[36] postulated that for a sample above ϕ_c and in the low-frequency regime $\omega < \omega_c$, $\tan\delta$ varies as $\tan\delta \propto 1/\omega RC$, thus predicting a slope of -1 (or $z=1$). In this calculation, it was assumed that the energy loss in the dielectric was only due to conduction along the backbone, which is known not to be true where there is a large $\varepsilon_{ri}(\omega)$ such as in the talc wax. Results obtained in the cellular systems, for samples just above the percolation threshold, give the slopes from -0.92 to -0.79 (or $z=0.79$–0.92) as shown in Table III, which do not agree with the predicition of Chen and Johnson.[36] The results from the cellular systems also show that the low-*t* systems give higher values of *z* than those with high *t*.

The loss angle at $\phi_c(\delta_c)$ has been found experimentally for all systems showing a minimum in $\tan\delta$, with δ_{ce} (experimental δ_c) being taken at this point (minimum) for a sample close to but below ϕ_c. In systems with no minimum in $\tan\delta$ (carbon black systems), the value of δ_{ce} was taken at 10^5 Hz. These results are shown in Table III.

Clerc *et al.*[3] predicted that δ_c is given by the expression $\delta_c = (\pi/2)(1-u) = (\pi/2)v = (\pi/2)[s/(s+t)]$, for $\omega \ll \omega_0 \equiv \sigma_c/2\pi\varepsilon_0\varepsilon_i$, which is true if the intercluster polarization model were obeyed. According to Clerc *et al.*,[3] the value of δ_c should depend only on the dimensionality of the system and has a value of 0.54 in three dimensions, when *s* and *t* are universal. Using the experimental dc exponents, values of $\delta_c(\delta_{ct})$ were calculated from $\delta_{ct} = (\pi/2)[s/(s+t)]$. Values of δ'_{ct} were obtained when s' (1 kHz) was used in place of *s* in the expression for δ_{ct}. The values of δ_{ce} for the cellular systems are all, except one, much greater than the δ_{ct} and δ'_{ct} values, as well as the universal 3D value of 0.54. It is not

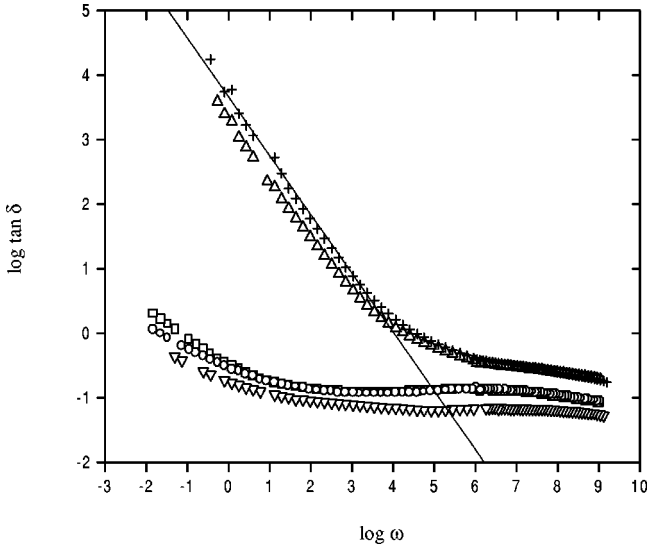

FIG. 15. A log-log plot of tan δ against ω for the raw carbon black system. The solid line is a linear fit to the data from a sample above ϕ_c which gives the value of the exponent z (from tan $\delta \propto \omega^{-z}$) to be $z=0.91\pm0.02$ [$\phi=0.01044$ (∇), $\phi=0.01290$ ($\bigcirc$), $\phi=0.01291$ ($\square$), $\phi=0.01334$ (Δ), $\phi=0.01343$ ($+$), with $\phi_c=0.0131\pm0.0006$].

clear what gives rise to such a serious discrepancy between the present experimental and calculated results. The previous results on graphite–boron-nitride systems studied by Wu and McLachlan[6] gave $\delta_{ce}=0.22\pm0.02$, 0.13 ± 0.02, and 0.09 ± 0.02 for the graphite–boron-nitride disks, 50% graphite, and 55% graphite–boron-nitride powder mixtures, respectively, which were also in disagreement with but less than the calculated values of δ_{ct} (δ'_{ct}).

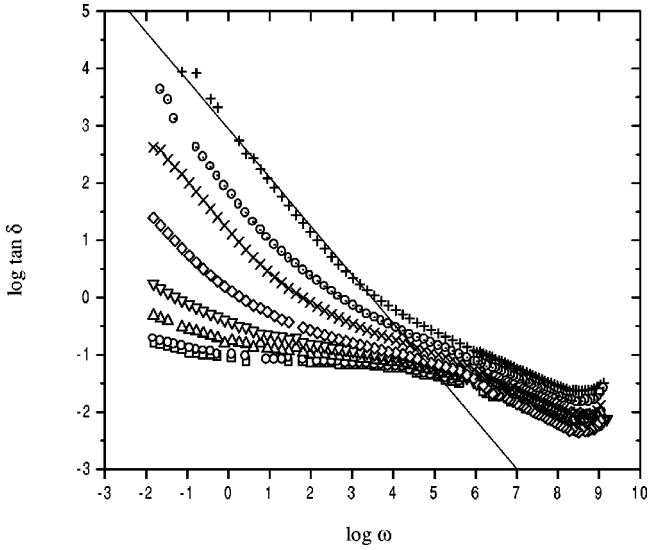

FIG. 16. A log-log plot of tan δ against ω for the Fe_3O_4 system. The solid line is a linear fit to the data from a sample above ϕ_c which gives the value of the exponent z (from $\tan\delta \propto \omega^{-z}$) as $z=0.85\pm0.02$ [$\phi=0.0219$ ($\square$), $\phi=0.0251$ ($\bigcirc$), $\phi=0.0281$ (Δ), $\phi=0.0344$ (∇), $\phi=0.036$ ($\diamond$), $\phi=0.0485$($\times$), $\phi=0.0627$ ($\odot$), $\phi=0.0840$ ($+$), with $\phi_c=0.025\pm0.003$].

Table III also shows the values of δ_{cu} and δ_{cv} calculated from the measured u_e and v_e, respectively, using $\delta_c=(\pi/2)(1-u)=(\pi/2)v$. These values are usually much lower than δ_{ce} and somewhat lower than δ_{ct} and δ'_{ct} in Table III, which indicates that it is the v_e values which are too low to give $u_e+v_e=1$ discussed earlier. This might be a characteristic of the cellular systems or a result of the complex dielectric properties of the talc-wax insulating component.

Other topics. We conclude this subsection with a few brief observations. The first is that when the real dielectric constant $\varepsilon_{mr}(\phi, \omega)$ results (below and close to ϕ_c) of the cellular systems were plotted as log-log plots of $\varepsilon_{mr}(\phi, \omega)$ versus frequency (10^{-2}–10^9 Hz), the respective dielectric constants of all systems decrease with frequency and appear to be converging towards the same value at very high frequencies. It is concluded that the dielectric behavior below the percolation threshold (ϕ_c) in all seven systems (including the nickel system) is dominated by the talc-wax insulating component, which is highly dispersive. Therefore no results or discussion is given because the results are dominated by the talc-wax dispersion and not the percolation properties.

The three-component system, containing some boron nitride, shows less dispersion than the other systems, as the talc wax in the $\phi=0.00$ sample is always coated by the more insulating and less dispersive boron nitride. Recall that the conducting graphite progressively replaces the boron nitride coating as the volume fraction of the former is increased from 0.00 to 0.15. These results are presented in detail in Ref. 39.

For completeness and a brief comparison, the same parameters as given in Table III, obtained from the previous experiments[6,7,35,36,38] in which the largest number of parameters were measured, are given in Table IV. Points to note are the following: In spite of the fact that some of the systems detailed in Table IV have rather different ϕ_c values, the range of t values is somewhat similar. Using this and other data no clear correlation between ϕ_c and t could be observed. The very limited amount of s and $s'(\omega)$ data shows a serious gap in previous experimental work. Despite the disagreements between u_e, u_t, and u'_t, experimental values of $u(u_e)$ measured on the cellular systems are in reasonable agreement with some previous studies on other 3D continuum percolation systems as can be seen from Tables III and IV. The results for the low-t systems in Refs. 6 and 36 and the present low-t systems all show good agreement between u_e and u'_t.

$1/f$ noise measurements have also been made on the GCB, RCB, GG, and GBN systems.[40] The results are rather complex, indicating a very complex LNB-type system just above ϕ_c. The model given in Ref. 40 for the noise parameters observed could also be an explanation for the high-t values observed for the Fe_3O_4 and NbC systems.

A number of graphs were plotted in order to find if there are any correlations between the various exponents given in Tables I and III. No definite trends were observed in these graphs. However, these graphs are available on request and appear in Ref. 39.

TABLE IV. Parameters from previous studies on percolation systems. The s' values in this table, from previous work by other workers, were measured at 1 kHz. G/BN(D), graphite–boron-nitride disks; G/BN(50% P), 50% graphite–50% boron-nitride powder; NI/FPP, filamentary nickel in polypropylene; NI/N, nodular nickel in polypropylene; C/W, carbon in wax.

	G/BN(D) [a]	G/BN(50% P) [a]	NI/FPP [b]	NI/NPP [b]	C/W [c]
ϕ_c	0.150 ± 0.001	0.120 ± 0.001	0.08 ± 0.01	0.28 ± 0.02	0.0076
s	1.01 ± 0.05	0.42 ± 0.01			
s'	0.53 ± 0.07	0.60 ± 0.01	0.55 ± 0.01	0.62 ± 0.01	
t	2.63 ± 0.07	4.85 ± 0.46	3.1 ± 0.3	2.2 ± 0.1	2.1

[a]References 6 and 7.
[b]Reference 36.
[c]Reference 35.

V. SUMMARY AND CONCLUSIONS

The first objective of this paper was to measure the electrical transport properties of a new class of percolation systems—namely, cellular systems—and to examine the percolation parameters of these systems to try to ascertain which microstrutural features were causing the nonuniversal exponents in these (and other) systems. As these cellular systems have low-ϕ_c values and very similar microstructures, any differences in the parameters must be due to the properties of the different conducting powders. A second objective was to check the validity and ability of standard percolation theory and a phenomenological equation [Eq. (1)] to fit or model the results for various ac and dc transport properties in terms of the standard percolation parameters and the scaling properties of these equations. Conclusions on these objectives are given below.

The geometries chosen also allowed one to examine the Kusy equation's ability to model the results for ϕ_c in such systems. The conclusion on this aspect of the paper is that the Kusy equation, which is based on monosized spherical conducting powder particles, does not accurately fit the results for real powders. However, it does appear to work better for the more spherical powders, where the grains make good contact with each other.

As Eq. (1) was found to fit the dc data (real and first order terms only) for *all* ϕ values, in this as well as other percolation systems, and was shown to be a dc scaling function by varying σ_i/σ_c, it would appear to adequately describe dc percolation systems. Further experiments on systems with high-ϕ_c values and high values of σ_i/σ_c should be carried out, to see if Eq. (1) will model such systems. The standard power laws also fit the results and give the same exponents as Eq. (1), in the limits in which they are valid.

The first-order ac experimental results presented in this paper and summarized in Table III are the most comprehensive to appear in the literature and the results and exponents are in general agreement with previous studies on 3D continuum systems (Table IV). However, examination of the experimental errors in the tables of results shows that the agreement is not always very good. The conducting samples ($\phi > \phi_c$) all show the expected low-frequency independent plateau followed by a frequency-dependent conductivity at high frequencies. A plot of the normalized real ac conductivity $[\sigma_{mr}(\phi,\omega)/\sigma_m(\phi,0)]$ of the conducting samples close to ϕ_c against the normalized frequency (ω/ω_{c+}) show that the results can all be scaled and that the scaling exponents u_e all lie between 0.70 and 0.86 in the systems studied. Therefore one can conclude that, except for the systems which display a hook for $x_+ > 1$, Eq. (1) and the standard percolation equations (for $x_\pm \ll 1$ and $x_\pm \gg 1$ only) seem adequate to model the experimental results, if one accepts the fitting parameters which are not yet completely understood.

As shown in Figs. 11 and 12, the first-order imaginary conductivity σ_{mi} below ϕ_c also behaves as expected from Eq. (1) and the percolation equations. In Ref. 6 these data were of a sufficiently high quality to actually scale according to the procedure given in Sec. II. Therefore, at first sight it appears that the first-order ac data can be adequately modeled by Eq. (1) and the standard percolation power laws are obeyed. Unfortunately, as shown in Table III, there is a serious problem in that for some systems there are not adequate models (the intercluster polarization or RC model) to relate the dc exponents (s or s', t, and ϕ_c) with the ac exponents (u and v). Probably the most serious anomaly is that in most of the systems studied in this work, the respective experimental u_e and v_e exponents do not sum up to unity as they should $(u+v=1)$ and are therefore in serious disagreement with all current models. Although new experiments would be useful, new theoretical input is urgently required.

However, the frequency dependence of ϵ_{mr}, as evidenced by the different slopes for different frequencies on log-log plots of ϵ_{mr} against $(\phi_{ce}-\phi)$, shows that the standard percolation equations as given in Refs. 3–5 are correct, provided one accepts a frequency dependent s (Table I). This is a cause for great concern as a large number of experiments[3–5,36,37] have presented data as if s were frequency independent and that $s'=s$, as implied in Refs. 3–5. Measurements of the second-order ac conductivity (dielectric constant), made on these cellular and other systems,[7,8] revealed severe problems with the predictions of the standard percolation equations. Although not discussed in this paper, the standard percolation theory's inability to model $\epsilon_{mr}(\phi,\omega)$ above ϕ_c (Refs. 8 and 9) shows that standard theory is not able to fit these second-order results for real continuum composites and that, except in the ideal limits $\sigma_c=\infty$ or $\sigma_i=\omega\varepsilon_0\varepsilon_i=0$ (i.e., for dc measurements only),

standard percolation theory should be replaced by Eq. (1).[9] Reference 8 has clearly shown that the ω^2 dependence predicted for the second order conductivity (or dielectric loss) term by standard percolation theory, below ϕ_c, is not present and the same is almost certainly the case here. An expression for this conductivity term in the low-ϕ limit, derived from Eq. (1), is discussed in Ref. 8. Due to the large dielectric loss terms in the insulating component in this and other work, it has not been possible to clearly identify the contribution of the percolation clusters.

Although the data presented in this paper are the most comprehensive ever presented and it has been shown that Eq. (1) more than adequately fits most of this and other percolation system data, it has not proved possible to fully understand the resulting parameters (exponents) and their interrelationships. Therefore, one should also explain the exponents in terms of a combination of the random void model, link, node, and blob model, and tunneling (in this case point contacts) model.

The original random void model and its extensions are the most widely used in explanations for nonuniversal exponents and are based on the geometric structure of a continuous conducting component. In our case, one must visualize insulating spheres with filaments and blobs of the conductor filling the spaces between them. Therefore the important difference for the different cellular systems is that each powder gives rise to its own characteristic link, node, and blob pattern, on the surfaces of the insulator. The links and nodes take the place of the small conducting filaments in the RV or Swiss-cheese model. The maximum t value for the RV model is 2.5 and for the LNB model is 2.35. Table I therefore indicates that these models are adequate to explain the t values of all the systems, except those containing Fe_3O_4 and NbC.

The fact that $\sigma_{cf} > \sigma_{cb}$ for all systems indicates that there is an interparticle resistance, but where the range of these resistances is small, the original Kogut-Straley[11] model would indicate that this would not increase t significantly. Values of t over 3.0 can be accounted for by the Balberg model.[15,16] However, the authors believe that the high-t values over 3.0 are due to RV-type geometric factors, which in this case consist of LNB networks, plus a large range of interparticle resistances in the Fe_3O_4, NbC (which have very angular contacts), and G-BN powders.[7] Note that these are also the systems with the hooks in the dispersion plots (Fig. 8). Note too that the the small s values measured in these systems requires an explanation, especially as the basic Kogut and Straley model does not allow s values less than s_{un}. The range and values of s, s' (1 kHz), and t values in Tables I and IV (which contains data from noncellular granular systems) show that the mechanisms that determine s, s', and t in the cellular systems are probably also determining s, s', and t in all these very complex systems, which all, except that in Ref. 14, involve a granular conducting component.

Finally the authors hope that this work will encourage more experiments and, more importantly, new theoretical work to model the origin of the nonuniversal exponents and the relationships between these exponents, which will explain the inconsistencies that have been highlighted in this paper.

[1] R. Landauer, in *Electrical Transport and Optical Properties of Inhomogeneous Media*, edited by J.C. Garland and D.B. Tanner, AIP Conf. Proc. No. 40 (AIP, New York, 1978), p. 2.

[2] D.S. McLachlan, M. Blaskiewicz, and R. Newnham, J. Am. Ceram. Soc. **73**, 2187 (1990).

[3] J.P. Clerc, G. Girand, J.M. Langier, and J.M. Luck, Adv. Phys. **39**, 1 (1990).

[4] D.J. Bergman and D. Stroud, in *Solid State Physics, Advances in Research and Applications*, edited by H. Ehrenreich and D. Turnbull (Academic, San Diego, 1992), Vol. 46, p. 147.

[5] Ce-Wen Nan, Prog. Mater. Sci. **37**, 1 (1993).

[6] Junjie Wu and D.S. McLachlan, Phys. Rev. B **58**, 14 880 (1998).

[7] Junjie Wu and D.S. McLachlan, Phys. Rev. B **56**, 1236 (1997).

[8] D.S. McLachlan, W.D. Heiss, C. Chiteme, and Junjie Wu, Phys. Rev. B **58**, 13 558 (1998).

[9] W.D. Heiss, D.S. McLachlan, and C. Chiteme, Phys. Rev. B **62**, 4196 (2000).

[10] D.S. McLachlan, Physica B **254**, 249 (1998).

[11] P.M. Kogut and J.P. Straley, J. Phys. C **12**, 2151 (1979).

[12] B.I. Halperin, S. Feng, and P.N. Sen, Phys. Rev. Lett. **54**, 2391 (1985).

[13] S. Feng, B.I. Halperin, and P.N. Sen, Phys. Rev. B **35**, 197 (1987).

[14] S. Lee, Y. Song, W.T. Noh, X. Chen, and J.R. Gaines, Phys. Rev. B **34**, 6719 (1986).

[15] I. Balberg, Trends Stat. Phys. **2**, 39 (1998).

[16] I. Balberg, Phys. Rev. B **57**, 13 351 (1998).

[17] P.G. de Gennes, J. Phys. (France) Lett. **37**, L1 (1976).

[18] A. Skal and B.I. Shklovskii, Fiz. Tekh. Poluprovodn. **8**, 1568 (1974) [Sov. Phys. Semicond. **8**, 1024 (1975)].

[19] H.E. Stanley, J. Phys. A **10**, L211 (1977).

[20] A. Coniglio, J. Phys. A **15**, 3829 (1982).

[21] R. Fisch and A.B. Harris, Phys. Rev. B **18**, 416 (1978).

[22] D.J. Bergman, Philos. Mag. B **56**, 983 (1987).

[23] D.J. Bergman and A.K. Sarychev, Physica A **200**, 231 (1993).

[24] M. Rhode and H. Micklitz, Phys. Rev. B **36**, 7572 (1987).

[25] M. Rhode and H. Micklitz, Physica A **157**, 120 (1989).

[26] M.B. Heaney, Phys. Rev. B **52**, 12 477 (1995).

[27] R.P. Kusy, J. Appl. Phys. **48**, 5301 (1977).

[28] G.E. Pike, in *Electrical Transport and Optical Properties of Inhomogeneous Media*, edited by J. Garland and D.B. Tanner, AIP Conf. Proc. No. 40 (AIP, New York, 1978), p. 366.

[29] A. Malliaris and D.T. Turner, J. Appl. Phys. **42**, 614 (1971).

[30] I. Balberg, Phys. Rev. Lett. **59**, 1305 (1987).

[31] N. Deprez and D.S. McLachlan, J. Appl. Phys. **21**, 101 (1988).

[32] I. Balberg, C.H. Anderson, S. Alexander, and N. Wagner, Phys. Rev. B **30**, 3933 (1984).

[33] F. Carmona, P. Prudhon, and F. Barreau, Solid State Commun. **51**, 225 (1984).

[34] M.T. Connor, S. Roy, T.A. Ezquerra, and F.J.B. Calleja, Phys. Rev. B **57**, 2286 (1998).

[35] C.C. Chen and Y.C. Chou, Phys. Rev. Lett. **54**, 2529 (1985).
[36] I.G. Chen and W.B. Johnson, J. Mater. Sci. **26**, 1565 (1991).
[37] D.M. Grannan, J.C. Garland, and D.B. Tanner, Phys. Rev. Lett. **46**, 375 (1981).
[38] R.K. Charkrabarty, K.K. Bardhan, and A. Basu, J. Phys.: Condens. Matter **5**, 2377 (1993).
[39] C. Chiteme, Ph.D. thesis, University of the Witwatersrand, 2001.
[40] C. Chiteme, D.S. McLachlan, and I. Balberg, following paper, Phys. Rev. B **67**, 024207 (2003).